Supporting Information

Mn(I)-based photoCORMs for trackable, visible light-induced CO release and photocytotoxicity to cancer cells

Dulal Musib,[†]Md Kausar Raza,[‡]Martina Kh.[†]and Mithun Roy[*,†]

†Department of Chemistry, National Institute of Technology, Manipur, Langol 795004, Imphal (Manipur), India

‡Department of Inorganic and Physical Chemistry, Indian Institute of Science, Bangalore 560012 (India)

Table of Content

1. Experimental Section and Measurements Procedure.

1.1. Physical Measurements

Molar conductivity measurements were done by using a EUTECH INSTRUMENT CON 510 (India) conductivity meter. UV-vis and emission spectra for the complexes were recorded in Perkin-Elmer UV/VIS spectrometer and HITACHI F-7000 Fluorescence spectrophotometer respectively. Solid-phase FT-IR spectra were recorded using Perkin-Elmer UATR TWO FT-IR Spectrometer operating from 400 to 4000 cm^{-1}. NMR spectra were recorded on a Bruker Avance 400 (400 MHz) spectrometer, using $CDCl_3$and DMSO-$d_6$as solvent and tetramethylsilane (TMS) as the internal standard. Q-TOF ESI Mass spectra (MS) were recorded in Bruker Esquire 3000 Plus spectrophotometer (Bruker-Franzen Analytic GmbH, Bremen, Germany). Time-correlated single-photon-counting (TCSPC) spectrometer (Horiba Jobin Yovon) was used to perform fluorescence lifetime measurement in which nanosecond laser of 375 nm was used as the excitation source in the following decay kinetics and data were analysed by a bi-exponential fitting program using IBH DAS-6 decay analysis software considering reduced chi-square value. The absorbance reading of MTT assays was collected using a Molecular Devises VersaMaxtunable microplate reader. All Theoretical calculations (DFT or TD-DFT) on all the ligand and complexes were carried out using Gaussian 09 rev. A.02. The input files to Gaussian 09 were prepared with Gauss view 5.0.8. Schematic drawing of the compounds and IUPAC names of all the ligands (L^1-L^4) were obtained by using ChemDrawProfessional 15.

1.2. Photolysis experiments

IR, UV-visible and fluorescence spectroscopy studied Photo-induced release CO from the photoCORMs (**1-4**). The apparent rates (k_{CO}) of CO release from the complexes (**1-4**) dissolved in MeCNon exposure to the visible light (400-700 nm, 10 Jcm^{-2}) were measured by using 10mm path length quartz cuvette. The cuvette was placed at a distance of 1 cm from the light source. CO release was followed at a 350nm wavelength of respective complexes, and the log of the concentration of the complex was plotted against time.The absorbance versus time plots was fitted to the three parameters exponential equation $A(t) = A_\infty + (A_0 - A_\infty) \exp\{-k_{CO}t\}$, where A_0 and A_∞ are the initial and final absorbance values, respectively. The apparent rate of CO loss (kCO) was calculated from the ln(C) versus time (T) plot for each metal carbonyl complex.The apparent CO released also confirmed by myoglobin assay [1].

1.3. Luminescence Experiments

The luminescence spectra of the complexes (**1-4**) in acetonitrile at the concentration of 250μM were recorded in a quartz cuvette (1 cm x 1 cm) at room temperature. The complexes (**1-4**) were excited at 345 nm (**1**), 347 nm (**2**), 410nm (**3**) and 350 (**4**) respectively to obtain luminescence spectra.

1.4. Myoglobin assay

Myoglobin from equine skeletal muscle was dissolved in phosphate buffered saline (PBS, 100 mM, pH 7.4) and reduced by adding sodium dithionite. The concentration of the deoxymyoglobin (Mb) generated was calculated from the absorbance of the Soret band at 434 nm. Next, 1-4 in MeOH were added to Mb, and the absorbance was taken after 5 min to ensure that the myoglobin was still reduced. On the basis of the Mb concentration, we added a MeOH solution of complex-4 (50Mm) to the Mb solution, and the initial absorbance was taken within 1 min then the absorbance was taken after 30 min. Finally, Carbonyl myoglobin (Mb-CO) produced. A shift in λmax from 434 to 422 nm was observed in each case because

of the formation of the Mb-CO. Final concentrations of Mb-CO were assessed at 424 nm and compared to the initial Mb present in the solution to quantify CO release by each compound.

1.5. DFT and TD-DFT Calculations

Theoretical calculations on all the ligands (L^1-L^4) and complexes (**1**-**4**) were carried out with density functional theory (DFT) and time-dependent density functional theory (TD-DFT) by usingGaussian 09 rev. A.02[2]. The input files were prepared with Gauss view 5.0.8. The structures of all the complexes (**1**-**4**) and ligands (L^1-L^4) in their ground state was optimized at the B3LYP/GEN level by using 6-31G(d,p) basis set for H, C, N, O, S atoms and LANL2DZ basic set for Mn atom in the gaseous phase. Using the DFT and TD-DFT calculation were performed to predict the electronic spectrum, and photo-induced CO release at the photo-activated statesof the complexes. Gauss Sumwas used to calculate the fractional contributions of various groups to each molecular orbital and also the contribution of percentage metal and ligands character involve corresponding in the HOMO and LUMO orbital [3].

After optimization of complex-4 (DFT), we performed TD-DFT calculation using B3LYP/GEN level by using 6-31G(d,p) basis set for H, C, N,O,S atoms and LANL2DZ basic set for Mn(I) to understand the excited state chemistry of the complex-4. At first we optimized singlet 1^{st}, 2^{nd} 3^{rd} and 4^{th} excited state of the complex-4, then we assign most populated electronic excited state (3^{rd} excited state) based on experimental result. Further we optimized 1^{st}, 2^{nd} and 3^{rd} excited triplet state using same basis function. From the optimized results we assign that electron jump from 3^{rd} excited singlet state to 2^{nd} excited triplet state *via* inter system crossing (ISC) because the lower energy difference between these two corresponding states. We observe significant increase in bond length for one of the Mn(I)-CO bond. Based on the literature survey we assumed that the solvent molecule (H_2O) occupied that vacant position of the complex **4** and Mn(I) converted to Mn(II) then again we optimized

the proposed 1st and 2nd triplet excited state using same basis function. Finally we observed simultaneous elongation for all the remaining Mn(II)-CO bond along with the Mn(II)-N and Mn(II)-O bonds in 2nd triplet excited state. Such elongation in metal to ligand bond might led to disintegration of the complex **4** into Mn(II), ligands and CO. The final observation was supported by reference 39 in the manuscript.

1.6. Cell Culture, Cell Viability Assay and Flow Cytometry Analysis

The 3-(4,5-dimethylthiazol-2-yl)-2,5-diphenyltetrazolium bromide (MTT) assay was performed to determine the photocytotoxicity of the complexes (**1**-**4**) [4]. The MTT assay was based on the ability of mitochondrial dehydrogenases of viable cells in cleaving the tetrazolium rings of MTT with the formation dark purple, cell impermeable formazan crystals, soluble in DMSO which could be quantified from by UV-visible spectroscopy. Approximately, 5000 cells of human cervical carcinoma (HeLa) cells,were plated separately in two different 96 wells culture plate and incubated with the complexes and the ligands dissolved in 1% DMSO/Dulbecco's 6 modified Eagle's medium (DMEM) in a dose-dependent manner (0.78 to 50 μM) for 4 h in the dark. After 4 h of initial incubation in the dark, the media was removed and replaced with DPBS buffer. One set of the cells were exposed to visible light (0, 5, 15 and30 min exposure, λ = 400-700 nm, light dose = 10 J cm^{-2}) using a Luzchem Photoreactor (Model LZC-1, Ontario, Canada) fitted with 8 fluorescent white tubes of Sylvania make in one of the plates, whereas the other set was kept in the dark for 0.3 hunder similar experimental condition. After photo-exposure, the DPBS was removed and replaced with fresh medium and incubation was continued for a further period of 19 h followed by the addition of 5 mg/mL of MTT (25 μL) to each well and incubated for an additional 3 h. The media was removed entirely from the wells, and DMSO (200 μL) was

added. Absorbance was recorded at 570 nm using TECAN microplate reader. Cytotoxicities of the complexes (**1**-**4**) was measured as the percentage ratio of the absorbance of the treated cells to the untreated controls. The IC_{50} values were determined by nonlinear regression analysis (Graph Pad Prism 6). Data were obtained by using three independent sets of experiments done in triplicate for each concentration.Using the luminescent property of complex **4**, the CO release study was further done by using flow cytometric study. Human cervical carcinoma cells were seeded appropriately (3.0×10^5) in 6 well plates and cultured for 24 h. Complex **4**(30μM) was pre-incubated with HeLa cells in the dark for 4 h then washed twice with PBS buffer and finally time-dependent photoirradiation (0, 5, 15 and 30 min exposure, λ = 400-700 nm, light dose = 10 J cm^{-2}) were done keeping one identical set in the dark in the same condition. The assay was performed after 19 h of incubation, the cells were trypsinization, and a single cell suspension was prepared. The fluorescence (green fluorescence of Annexin V-FITC dye)of the cells was measured with a flow cytometer (FACS canto, Beckton Dickenson)[5].

References

1. M. A. Gonzalez, N. L. Fry, R. Burt, R. Davda, A. Hobbs, and P. K. Mascharak, Inorg. Chem., 50 (2011) 3127-3134.
2. (a) J. Full, L. Gonza´lez, C. Daniel, J. Phys. Chem. A 105 (2001) 184-189
3. (a) E. Üstün, M. S. Çelebi, M. Ç. Ayvaz, 2018, DOI: 10.1080/00958972.2018.1506110. (b)A. C. Merkle, N. L. Fry, P. K. Mascharak, N. Lehnert, Inorg. Chem.50 (2011) 12192-12203.
4. M. K. Raza, S. Gautam, P. Howlader, A. Bhattacharyya, P. Kondaiah, A. R. Chakaravrty,Inorg Chem. 57 (2018) 14374-14385.
5. (a) M. N. Pinto, I. Chakraborty, C. Sandoval, P. K. Mascharak, J. Control. Release, 264 (2017), 192-202. (b)M. Wächtler, J. Kübel, K. Barthelmes, A. Winter, A

Schmiedel, T. Pascher, C. Lambert, U. S. Schubert, B. Dietzek, Phys. Chem. Chem. Phys.18 (2016) 2350-2360.

Table S1. Selected Mn(I) to ligand bond length of the complex 4 at different excited states determined from DFT and TD-DFT calculations at TDDFT/B3LYP/6-31G(d,p)/LanL2DZ level.

Complex-4 States	Bond Length				
	Mn-N	Mn-O	Mn-CO[1]	Mn-CO[2]	Mn-CO[3]
Ground State (S_0)	1.8912	1.8605	1.9334	1.9418	1.9465
Excited State (S_1)	1.8912	1.8605	1.9334	1.9418	1.9465
Triplet State (T_1)	1.8909	1.8604	**1.9335**	1.9419	1.9467
Triplet State (T_2)	1.8909	1.8604	**1.9494**	1.9420	1.9467
Triplet State (T_2*)[a]	**1.9450**	**1.8943**	**1.8643**	**1.9562**	**1.9671**

[a]Refer to Figure 4. The bond lengths of concerned for photo-activated release of CO were made bold.

Table S2. MTT data of all complexes in visible light exposure (400-700 nm, 10 J cm^{-2}).

Complex	Dark **IC_{50} [µm]**	5 min. Light **IC_{50} [µm]**	15 min. Light **IC_{50} [µm]**	30 min Light **IC_{50} [µm]**
1	57.13	48.12	41.81	32.39
2	69.77	49.59	40.85	36.04
3	87.61	46.62	29.16	19.89
4	56.25	26.81	7.696	7.295

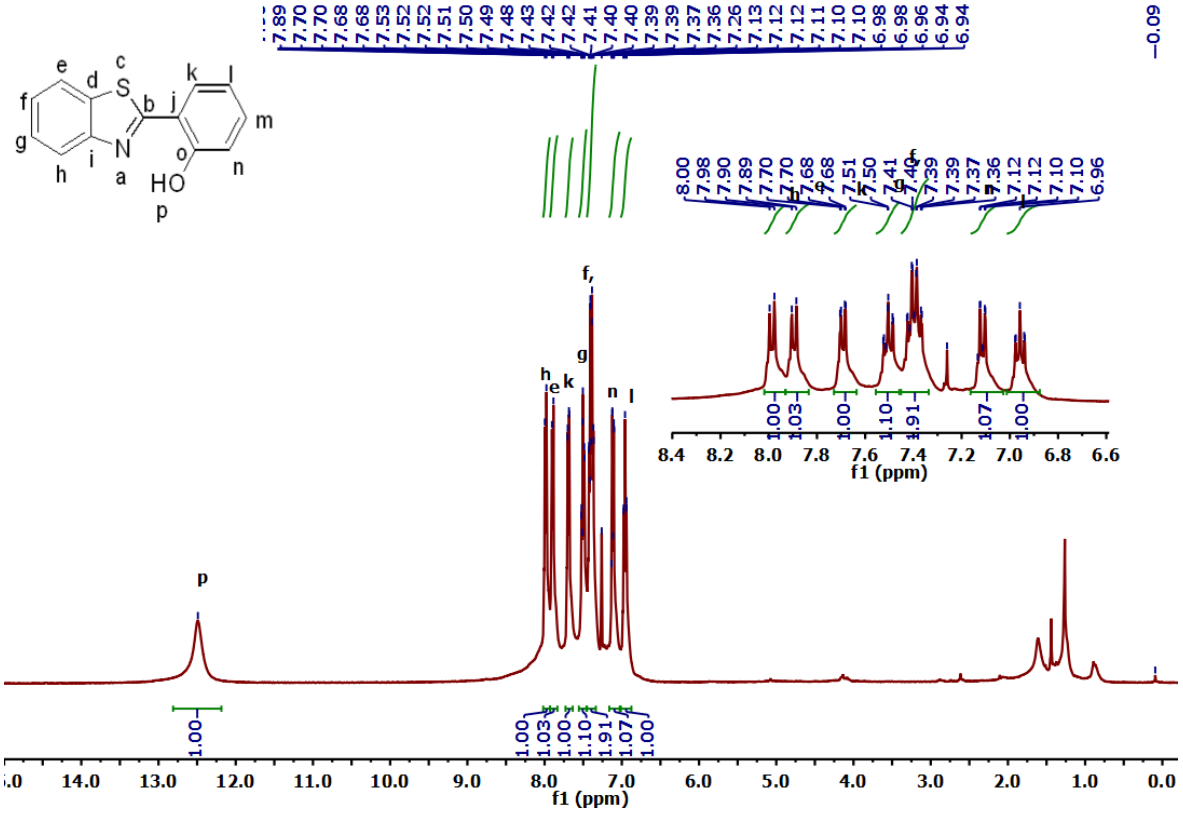

Figure S1.[1]H NMR of **L**[1] recorded in DMSO-d_6 using Bruker Avance 400 (400 MHz) spectrometer.

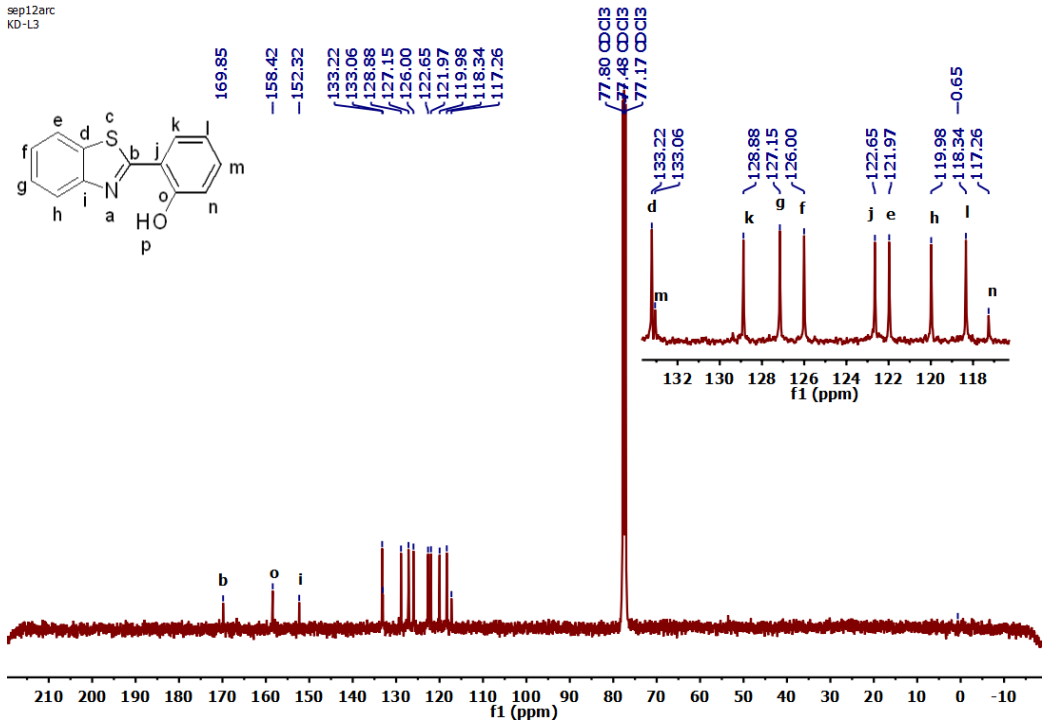

Figure S2.[13]C NMR of **L**[1] recorded in DMSO-d_6Bruker Avance 400 (100 MHz) spectrometer.

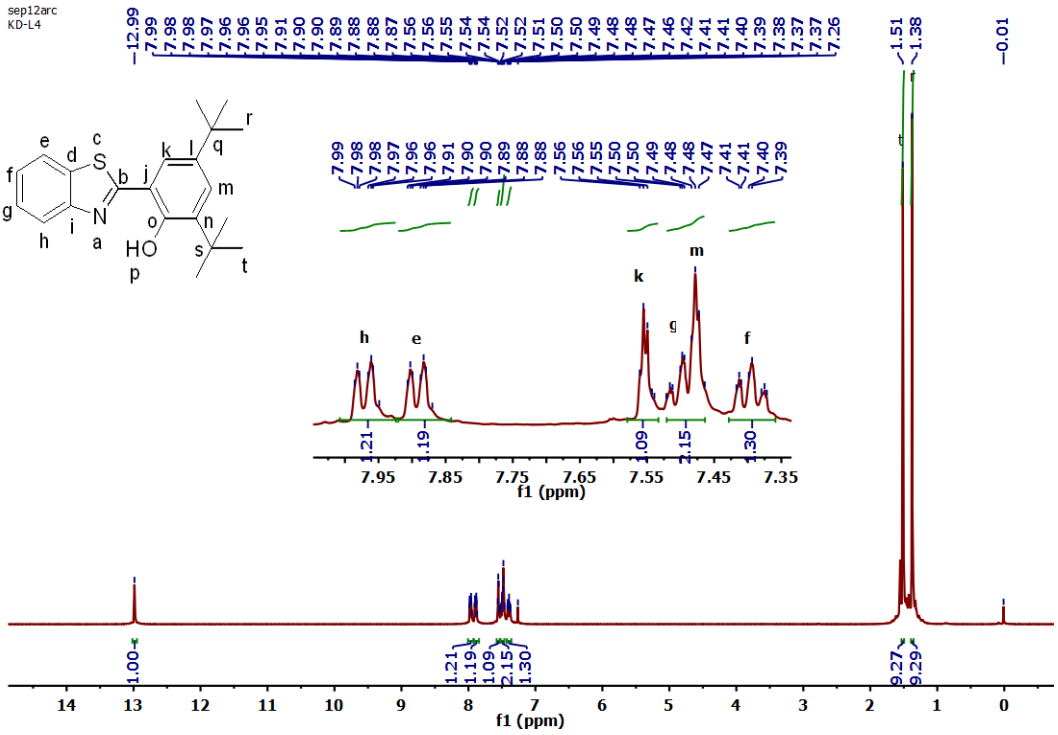

Figure S3.[1]H NMR of **L**[2] recorded in DMSO-d_6Bruker Avance 400 (400 MHz) spectrometer**.**

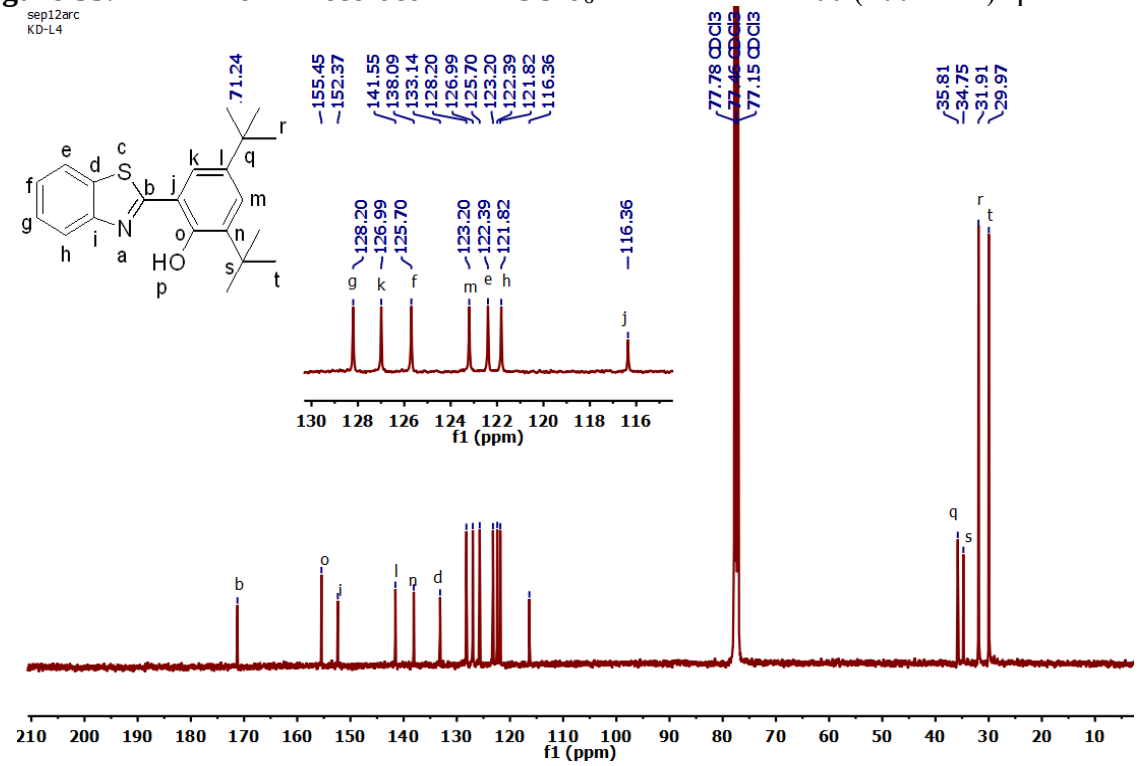

Figure S4.[13]C NMR of **L**[2] recorded in DMSO-d_6Bruker Avance 400 (100 MHz) spectrometer.

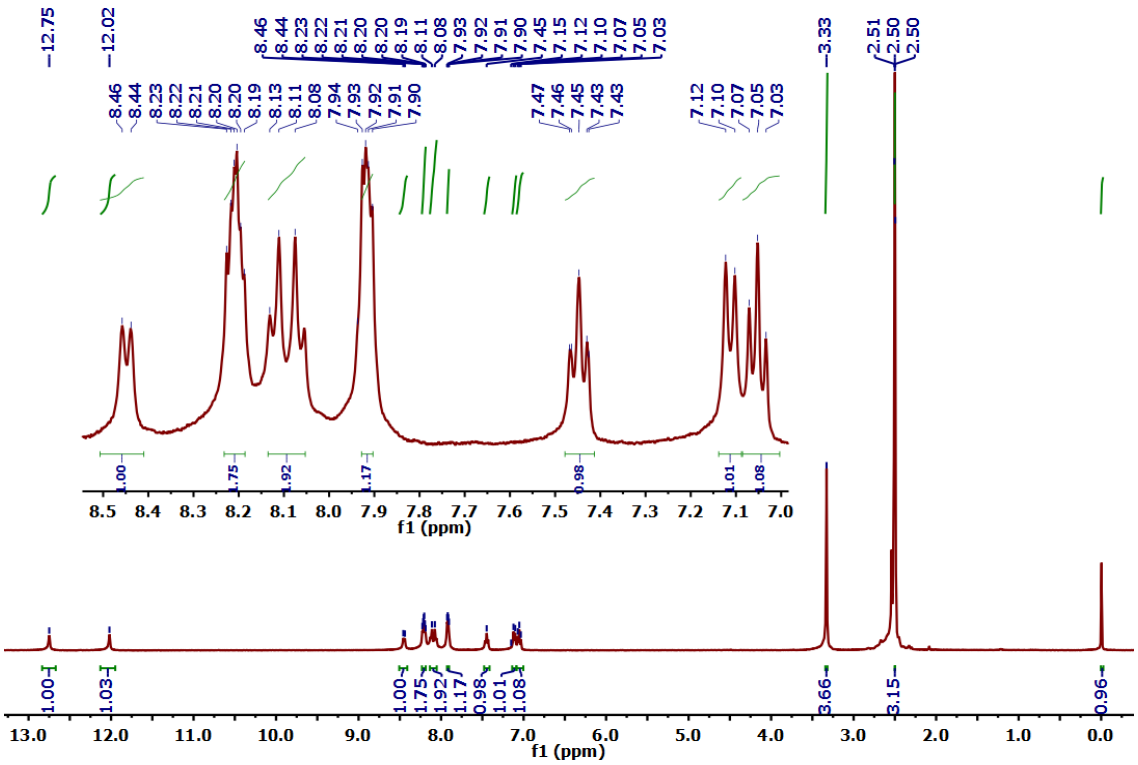

Figure S5.[1]H NMR of **L**[3] recorded in DMSO-d_6 Bruker Avance 400 (400 MHz) spectrometer**.**

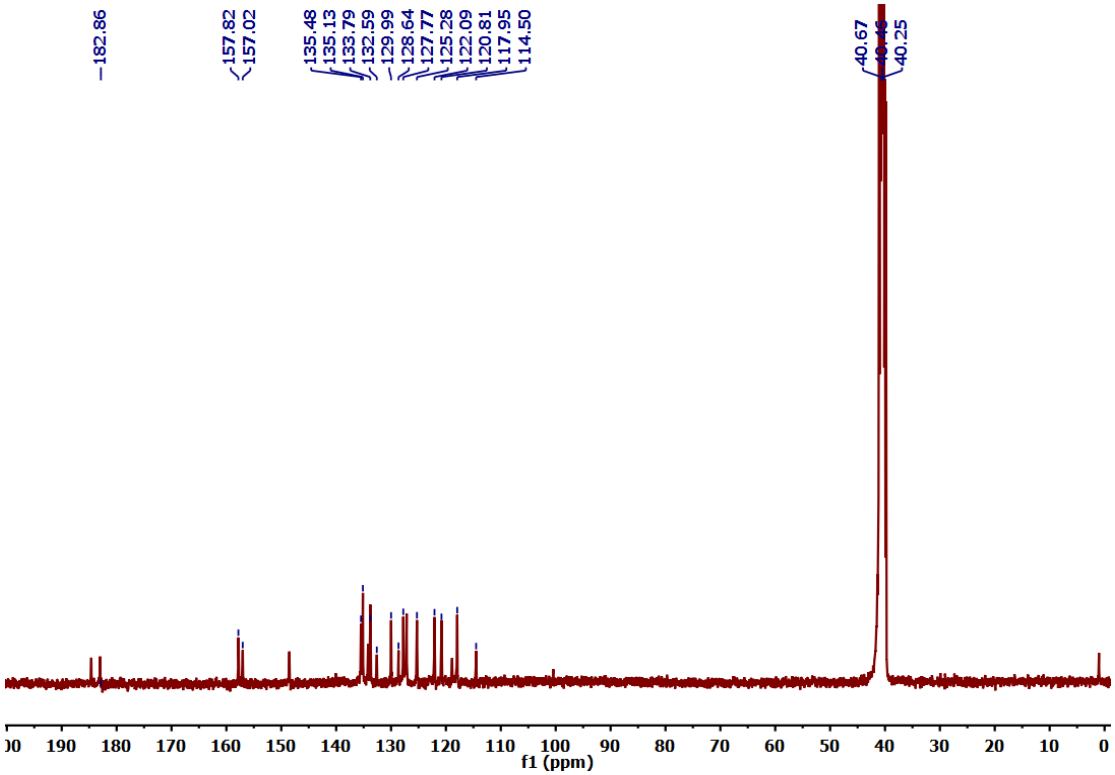

Figure S6.[13]C NMR of **L**[3] recorded in DMSO-d_6 Bruker Avance 400 (100 MHz) spectrometer.

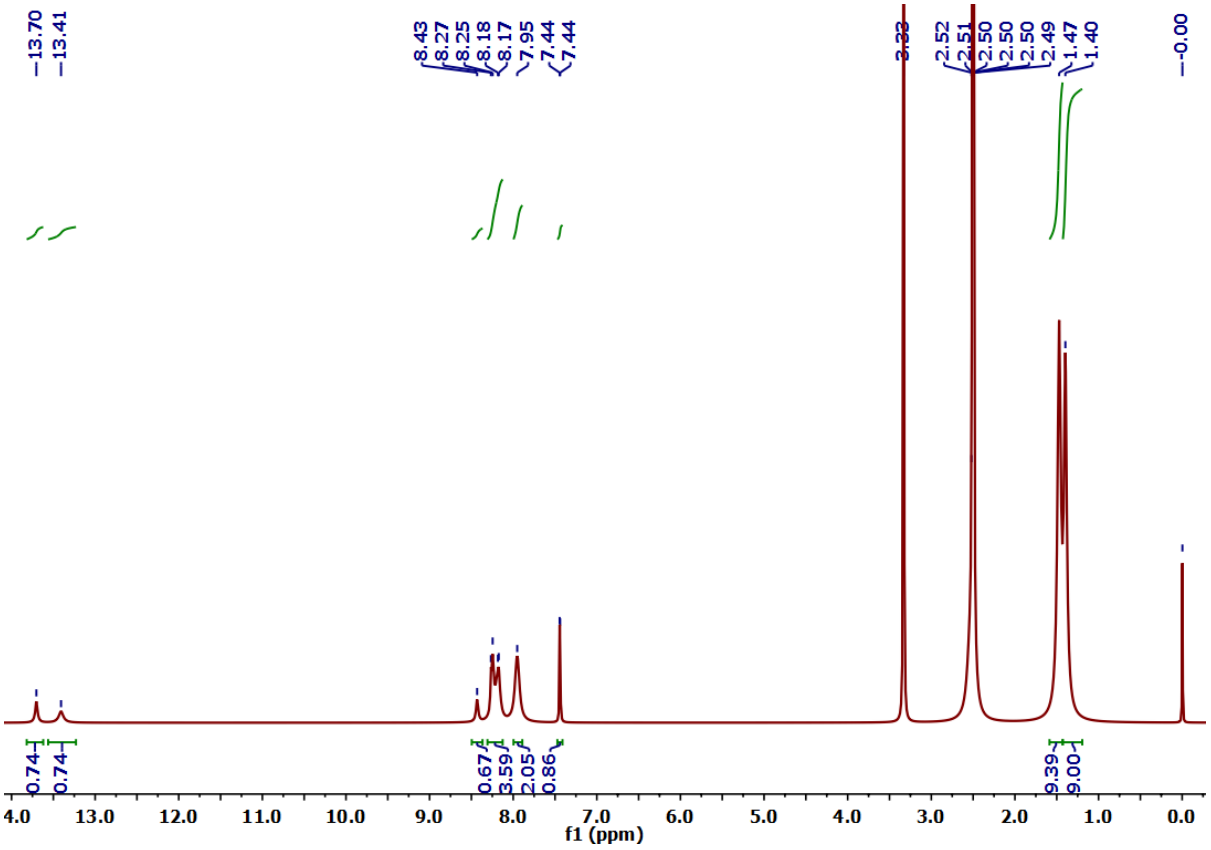

Figure S7.[1]H NMR of **L**[4] recorded in DMSO-d_6 Bruker Avance 400 (400 MHz) spectrometer**.**

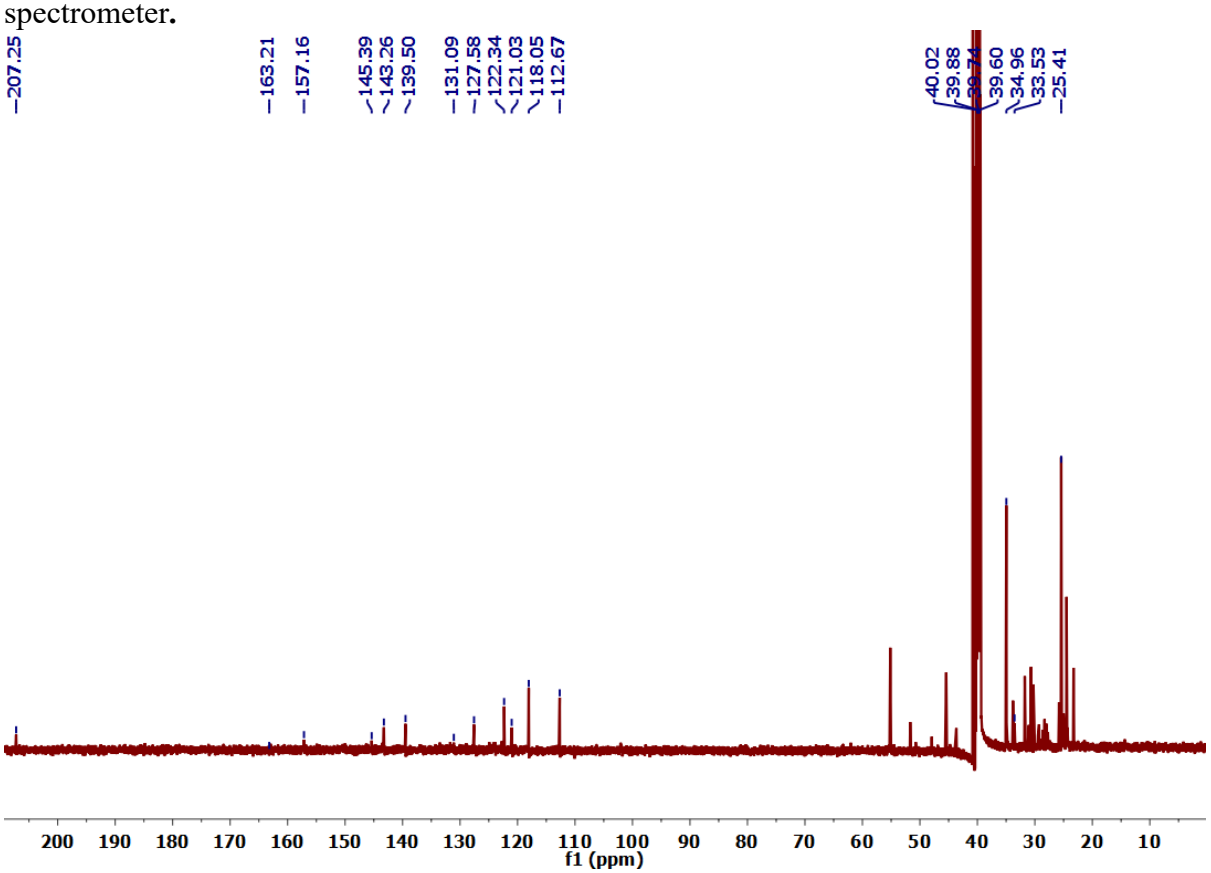

Figure S8. ^{13}C NMR of $\mathbf{L^4}$ recorded in DMSO-d_6 Bruker Avance 400 (100 MHz) spectrometer.

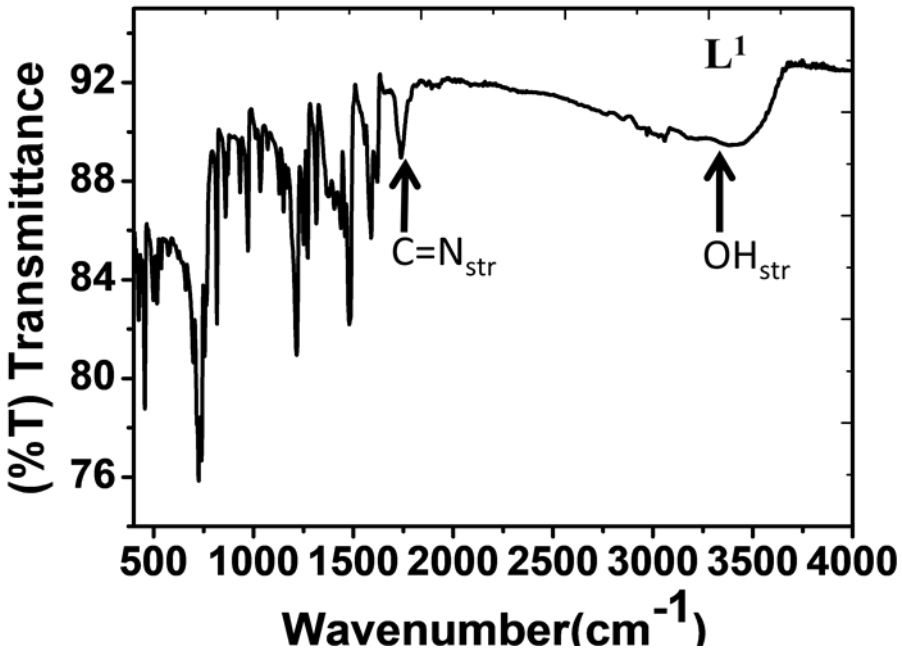

Figure S9. IR Spectra of $\mathbf{L^1}$ recorded in KBr phase using Perkin-Elmer UATR TWO FT-IR Spectrometer.

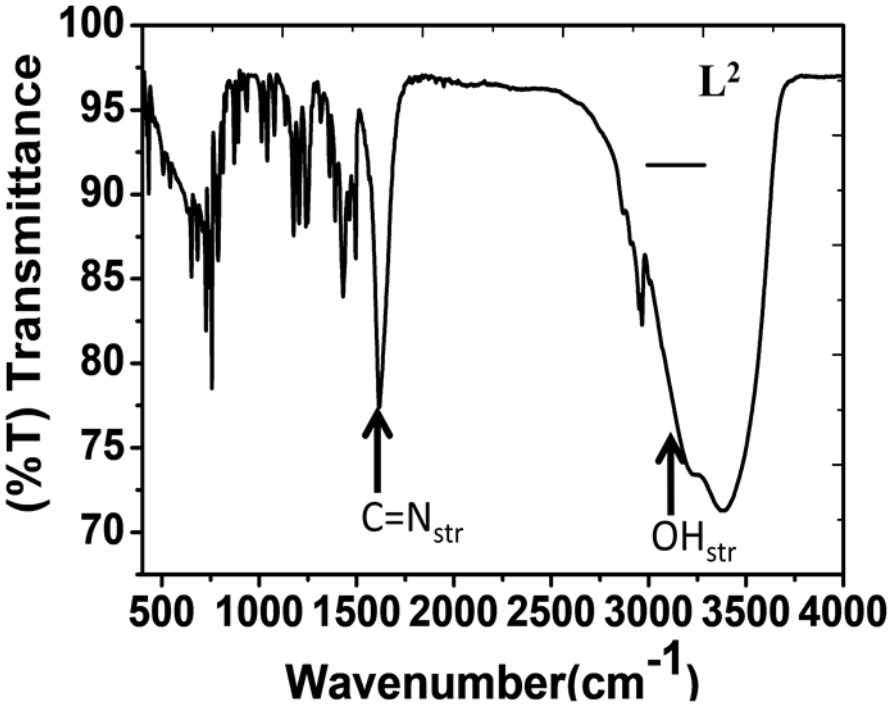

Figure S10. IR Spectra of $\mathbf{L^2}$ recorded in KBr phase using Perkin-Elmer UATR TWO FT-IR Spectrometer.

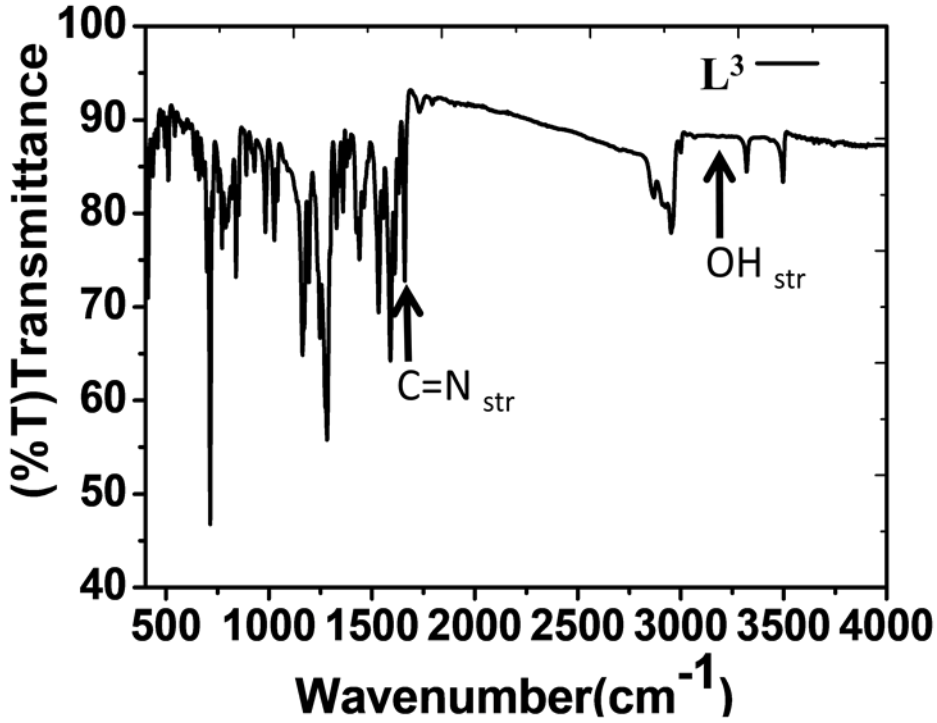

Figure S11. IR Spectra of **L^3** recorded in KBr phase using Perkin-Elmer UATR TWO FT-IR Spectrometer.

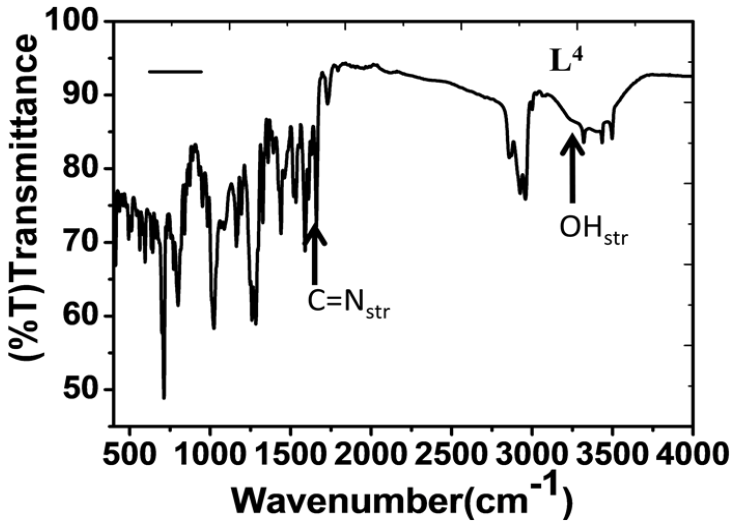

Figure S12. IR Spectra of **L^4** recorded in KBr phase using Perkin-Elmer UATR TWO FT-IR Spectrometer.

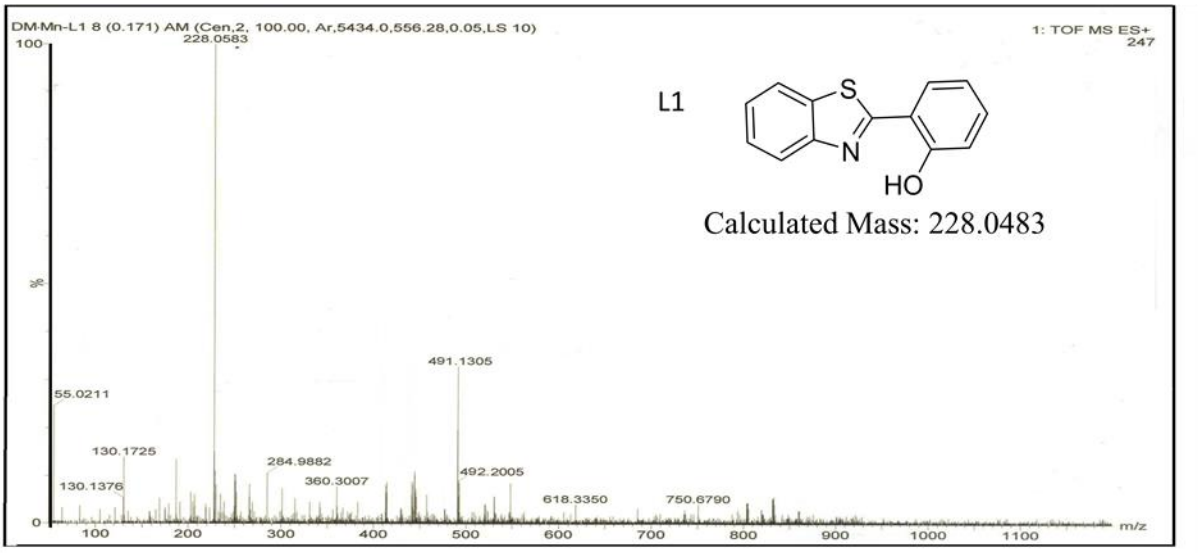

Figure S13. Q-TOF ESI Mass spectra of the **L[1]** recorded in CH_3CN usingBruker Esquire 3000 Plus spectro-photometer (Bruker-Franzen Analytic GmbH, Bremen, Germany). The peak at m/z 228.0556 corresponds to the species $[L^1H]^+$.

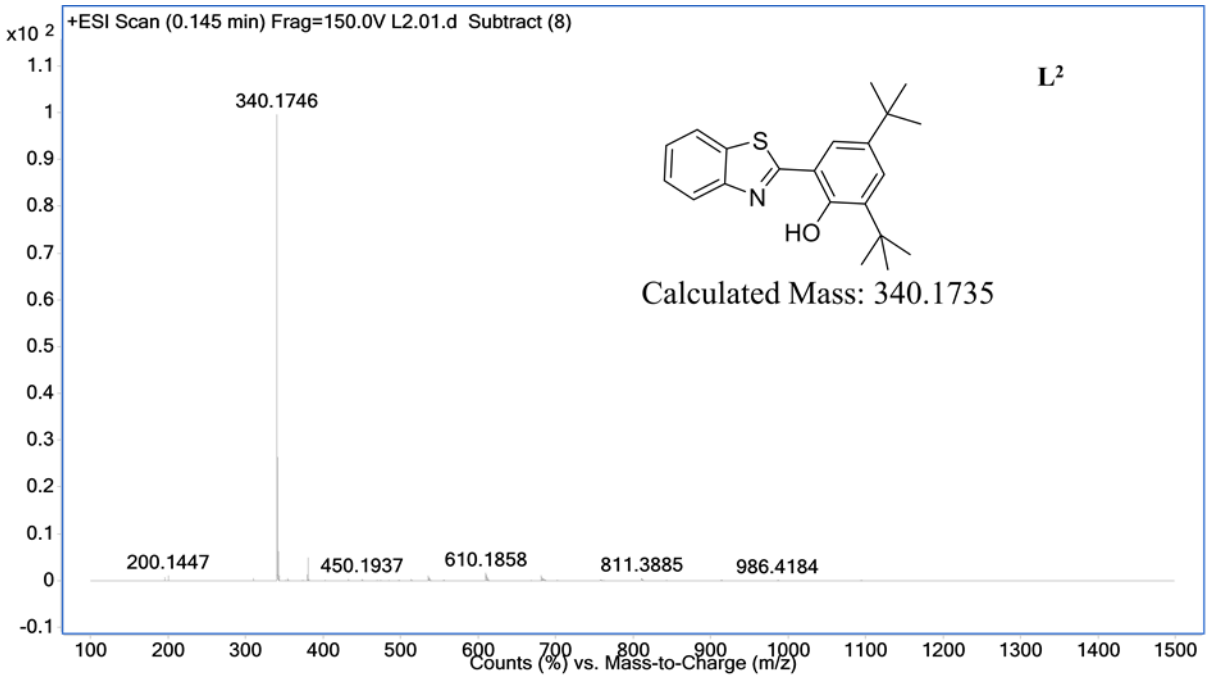

Figure S14. Q-TOF ESI Mass spectra of the **L[2]** recorded in CH_3CN usingBruker Esquire 3000 Plus spectro-photometer (Bruker-Franzen Analytic GmbH, Bremen, Germany). The peak at m/z 340.1746 corresponds to the species $[L^2H]^+$.

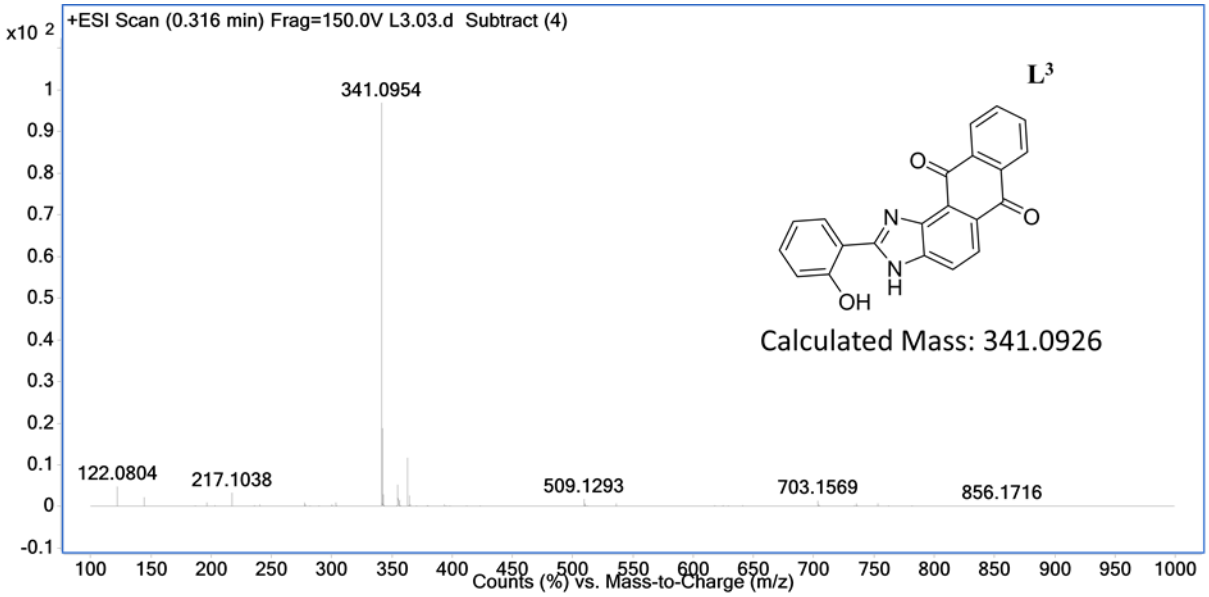

Figure S15. Q-TOF ESI Mass spectra of the **L^3** recorded in CH_3CN usingBruker Esquire 3000 Plus spectro-photometer (Bruker-Franzen Analytic GmbH, Bremen, Germany). The peak at m/z 341.0954 corresponds to the species $[L^3H]^+$.

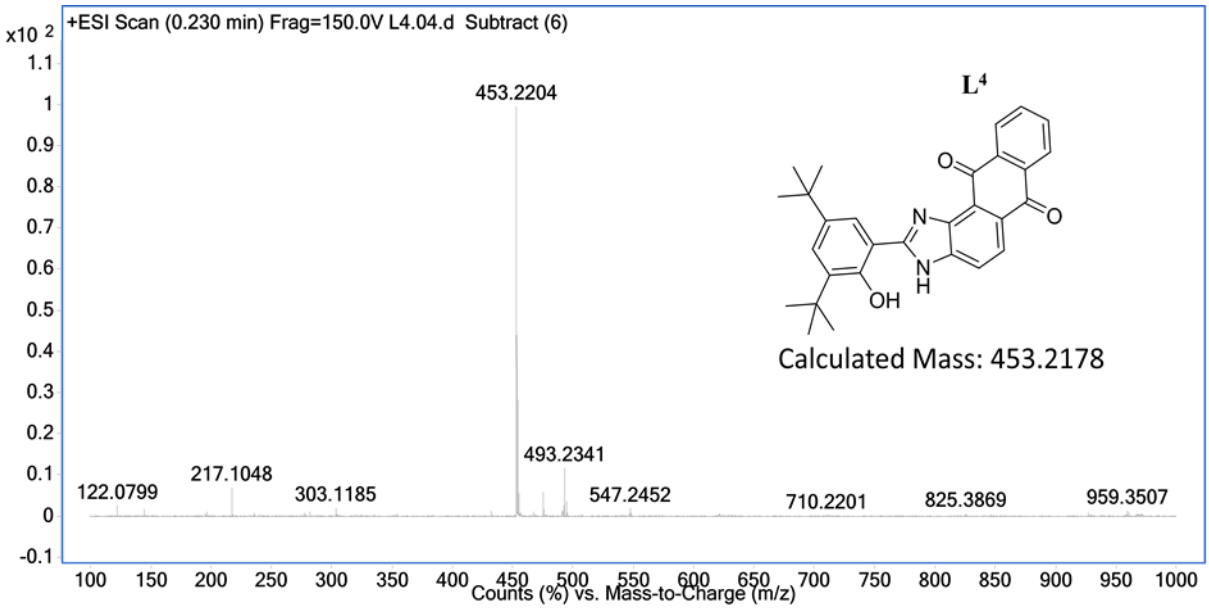

Figure S16. Q-TOF ESI Mass spectra of the **L^4** recorded in CH_3CN usingBruker Esquire 3000 Plus spectro-photometer (Bruker-Franzen Analytic GmbH, Bremen, Germany). The peak at m/z 453.2204 corresponds to the species $[L^4H]^+$.

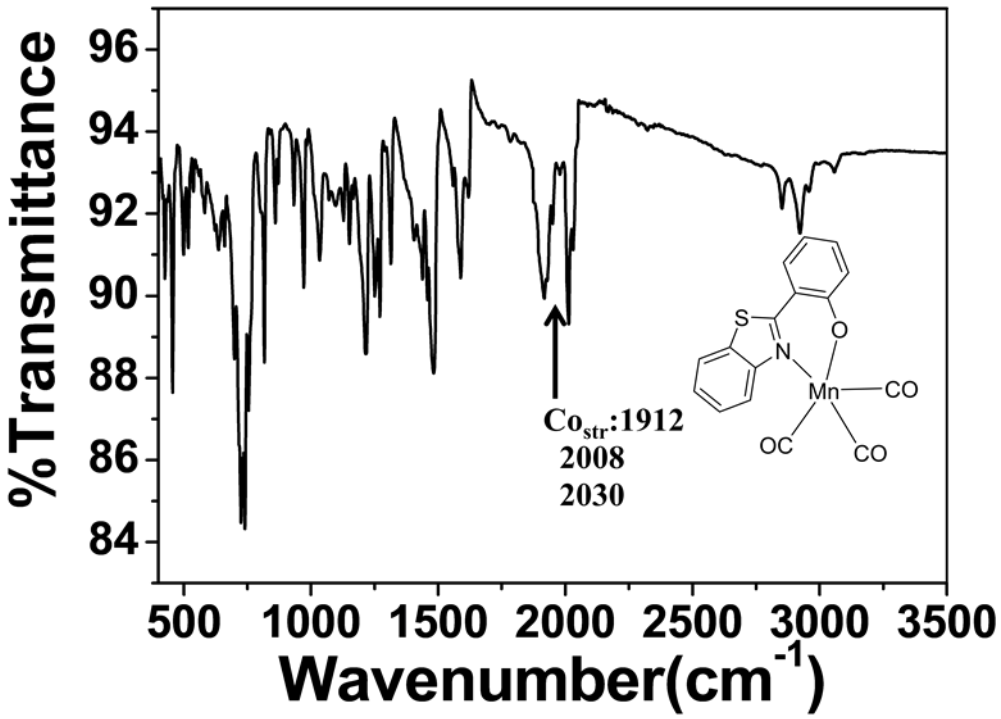

Figure S17. IR Spectra of **1** recorded in KBr phase using Perkin-Elmer UATR TWO FT-IR Spectrometer.

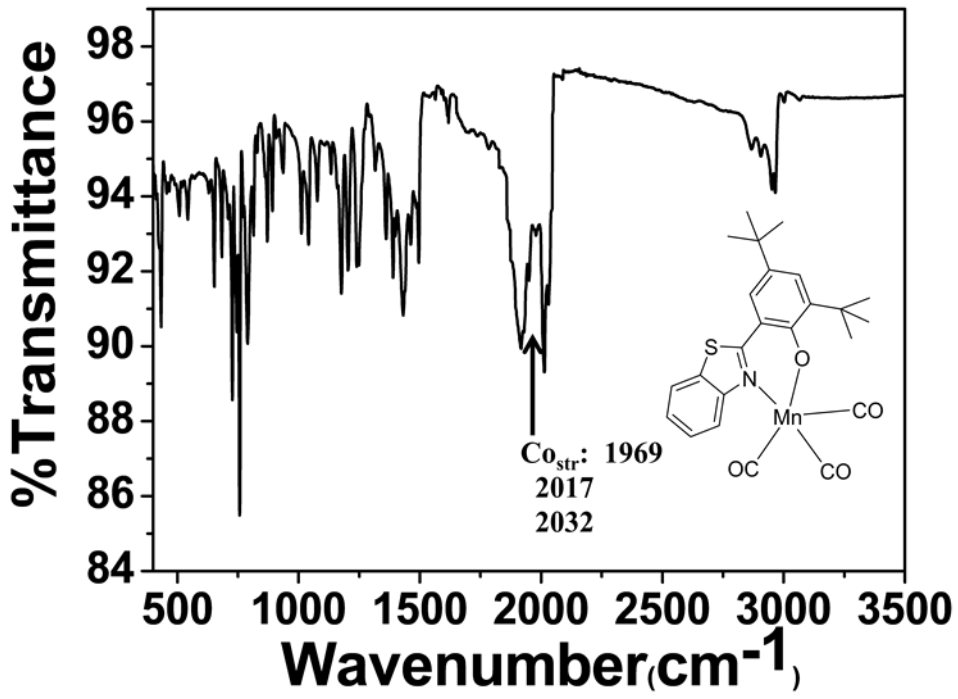

Figure S18. IR Spectra of **2** recorded in KBr phase using Perkin-Elmer UATR TWO FT-IR Spectrometer.

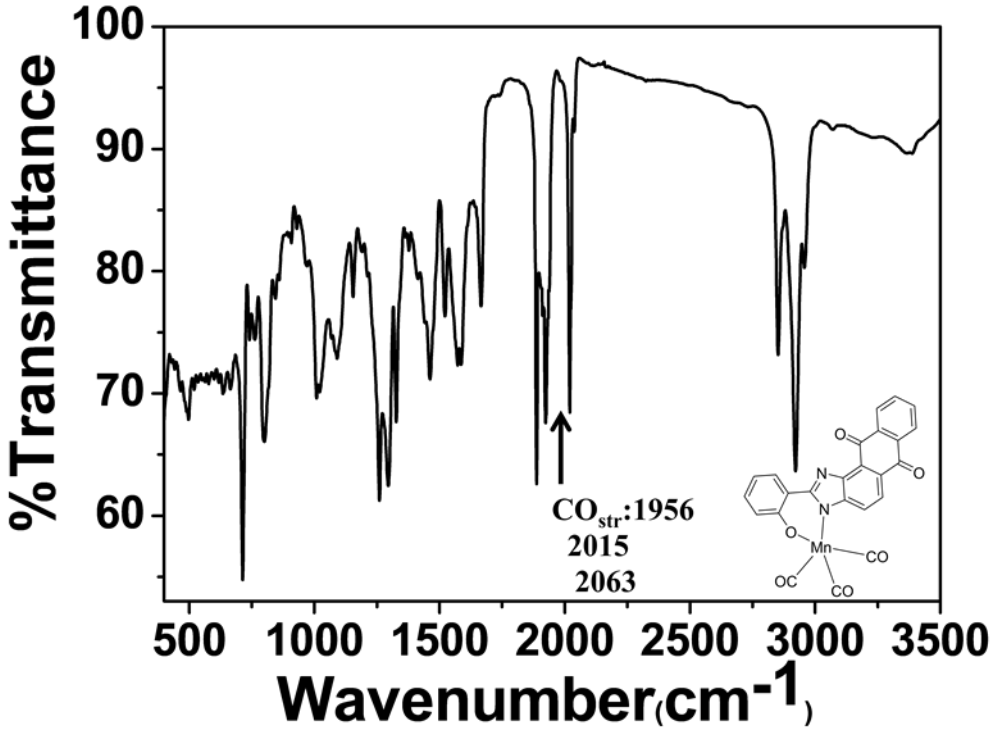

Figure S19. IR Spectra of **3** recorded in KBr phase using Perkin-Elmer UATR TWO FT-IR Spectrometer.

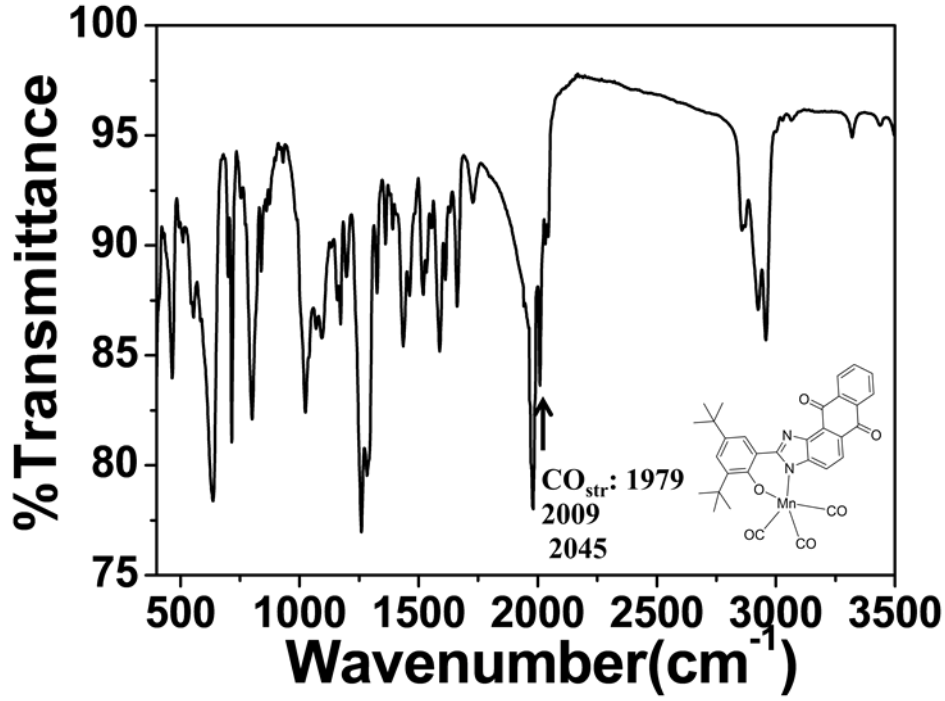

Figure S20. IR Spectra of **4** recorded in KBr phase using Perkin-Elmer UATR TWO FT-IR Spectrometer.

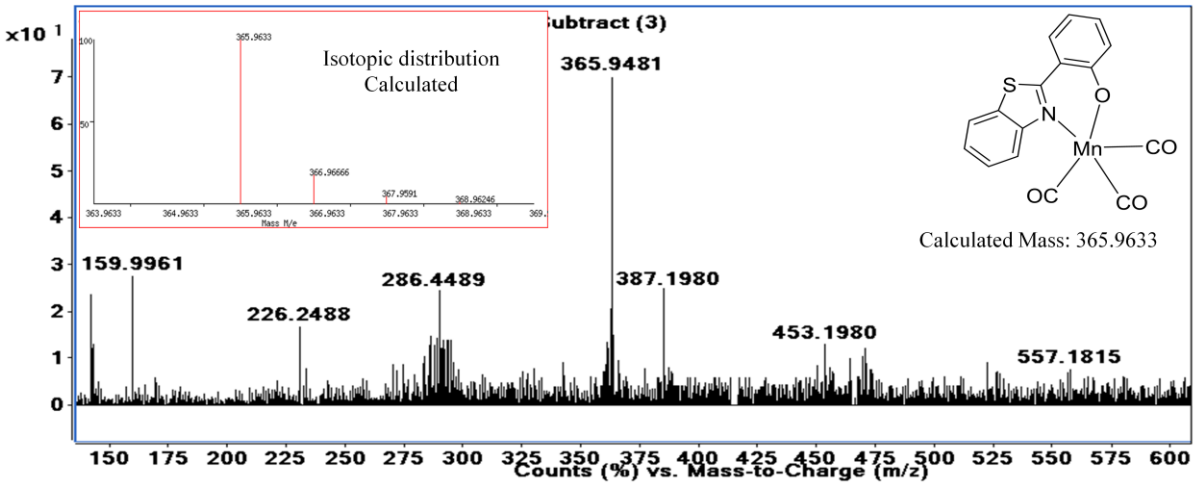

Figure S21. Q-TOF ESI Mass spectra of **1** recorded in CH_3CN using Bruker Esquire 3000 Plus spectro-photometer (Bruker-Franzen Analytic GmbH, Bremen, Germany). The peak at m/z 365.9481 corresponds to the species $[Mn(L^1)(CO)_3]H^+$ and m/z 387.1980 corresponds to the species $[Mn(L^1)(CO)_3]Na^+$. The inset represents the corresponding calculated isotopic distribution.

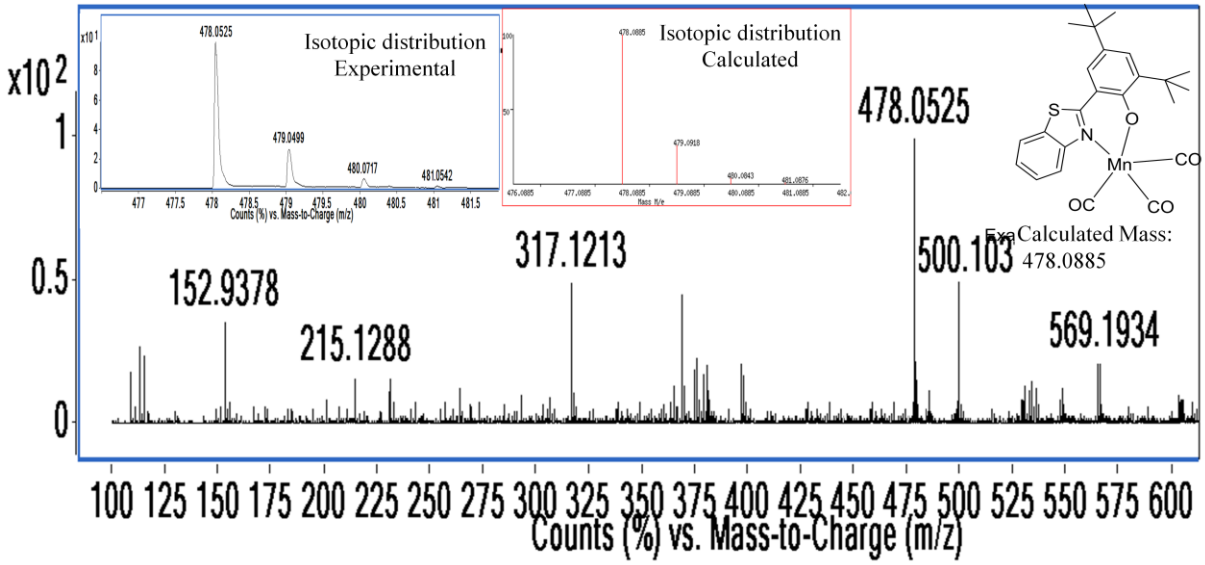

Figure S22. Q-TOF ESI Mass spectra of **2** recorded in CH_3CN usingBruker Esquire 3000 Plus spectro-photometer (Bruker-Franzen Analytic GmbH, Bremen, Germany). The peak at m/z 478.0525 corresponds to the species $[Mn(L^2)(CO)_3]H^+$ and m/z 500.1031 corresponds to the species $[Mn(L^2)(CO)_3]Na^+$. The inset represents the corresponding isotopic distribution (experimental and calculated).

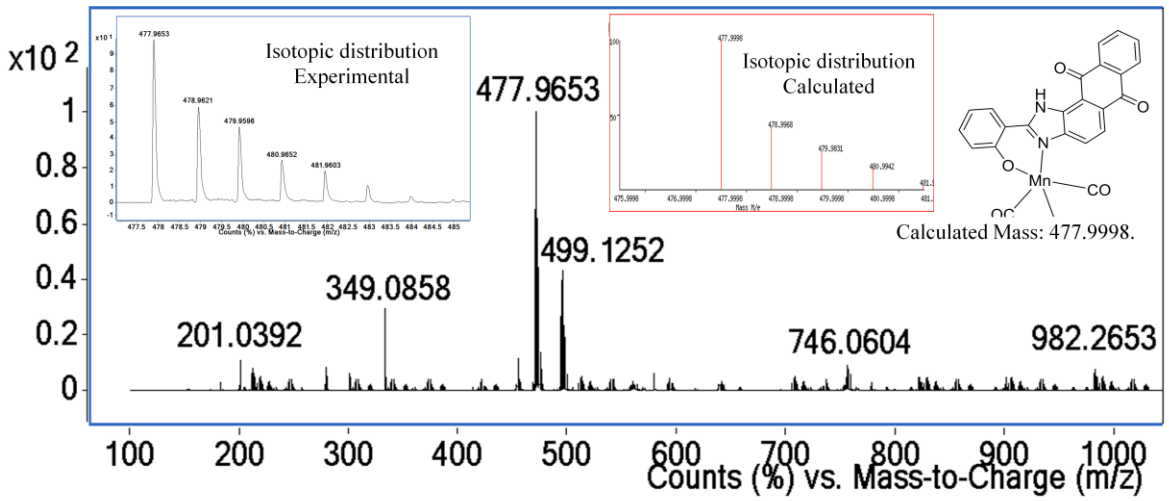

Figure S23. Q-TOF ESI Mass spectra of **3** recorded in CH_3CN usingBruker Esquire 3000 Plus spectro-photometer (Bruker-Franzen Analytic GmbH, Bremen, Germany). The peak at m/z 477.9653 corresponds to the species $[Mn(L^3)(CO)_3]H^+$ and m/z 499.1252 corresponds to the species $[Mn(L^3)(CO)_3]Na^+$. The inset represents the corresponding isotopic distribution (experimental and calculated).

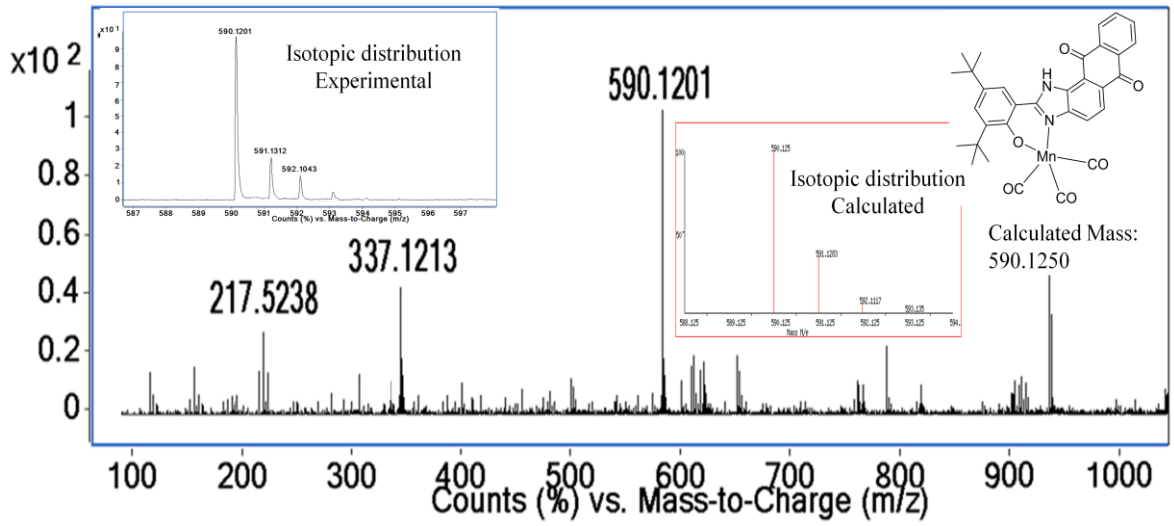

Figure S24. Q-TOF ESI Mass spectra of **4** recorded in CH_3CN usingBruker Esquire 3000 Plus spectro-photometer (Bruker-Franzen Analytic GmbH, Bremen, Germany). The peak at m/z 477.9653 corresponds to the species $[Mn(L^4)(CO)_3]H^+$. The inset represents the corresponding isotopic distribution(experimental and calculated).

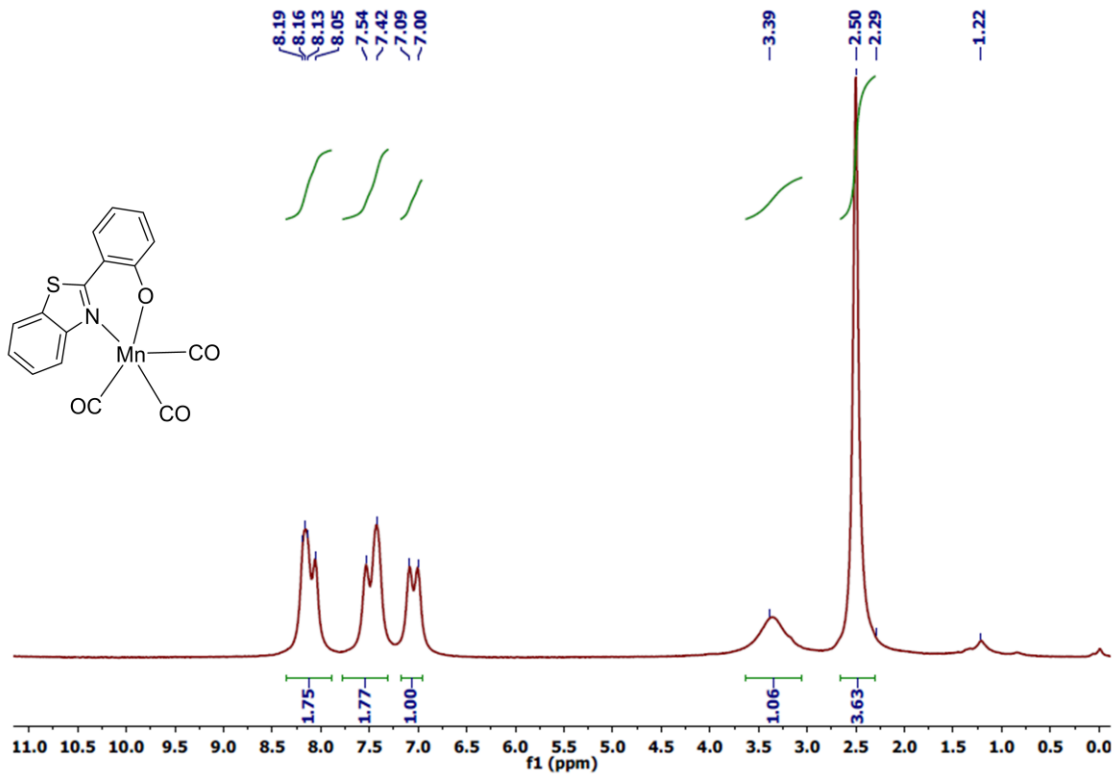

Figure S25.[1]H NMR of **1** recorded in DMSO-d_6 Bruker Avance 400 (400 MHz) spectrometer**.**

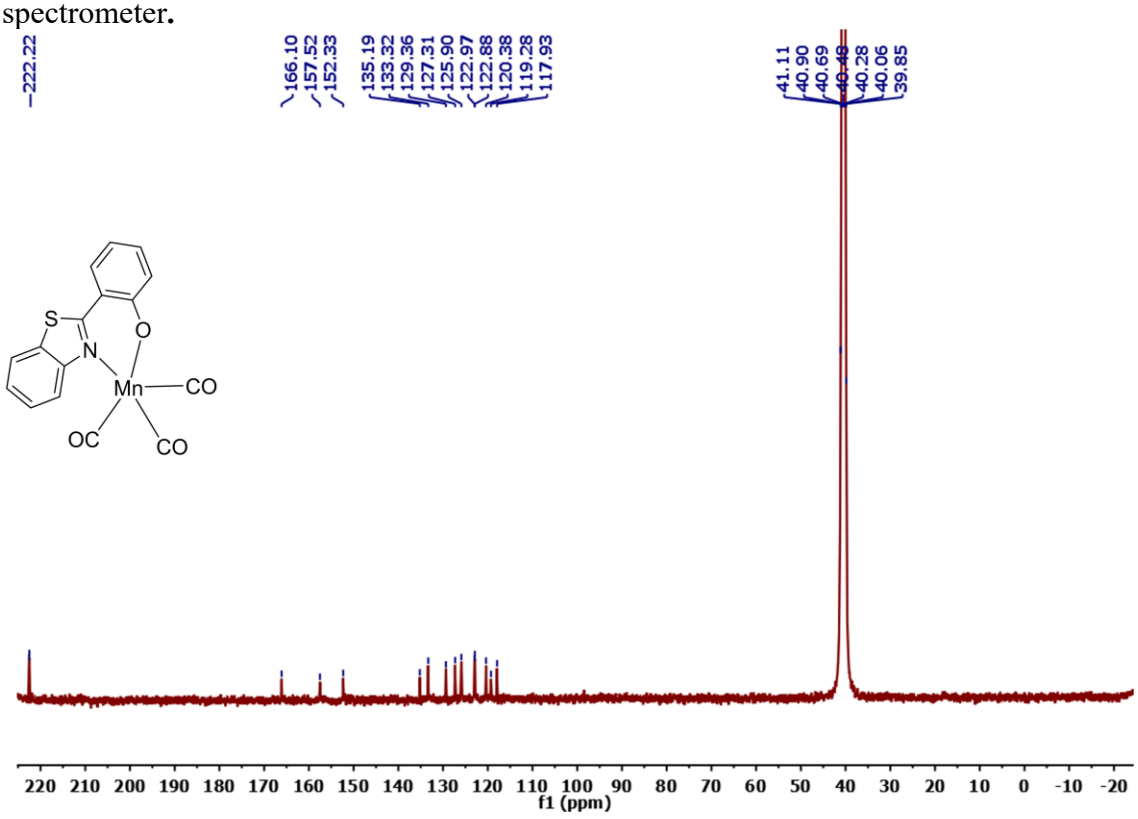

Figure S26.[13]C NMR of **1** recorded in DMSO-d_6Bruker Avance 400 (100 MHz) spectrometer.

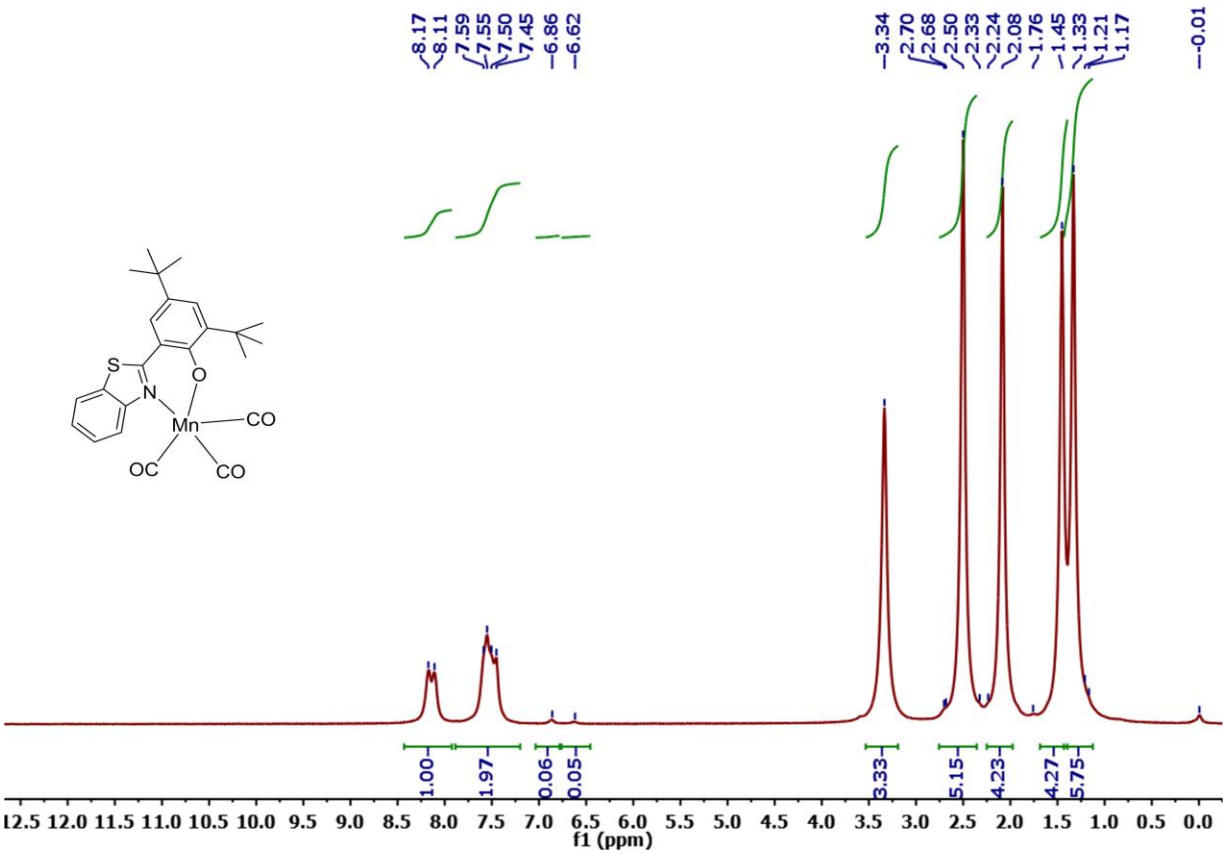

Figure S27.[1]H NMR of **2** recorded in DMSO-d_6 Bruker Avance 400 (400 MHz) spectrometer**.**

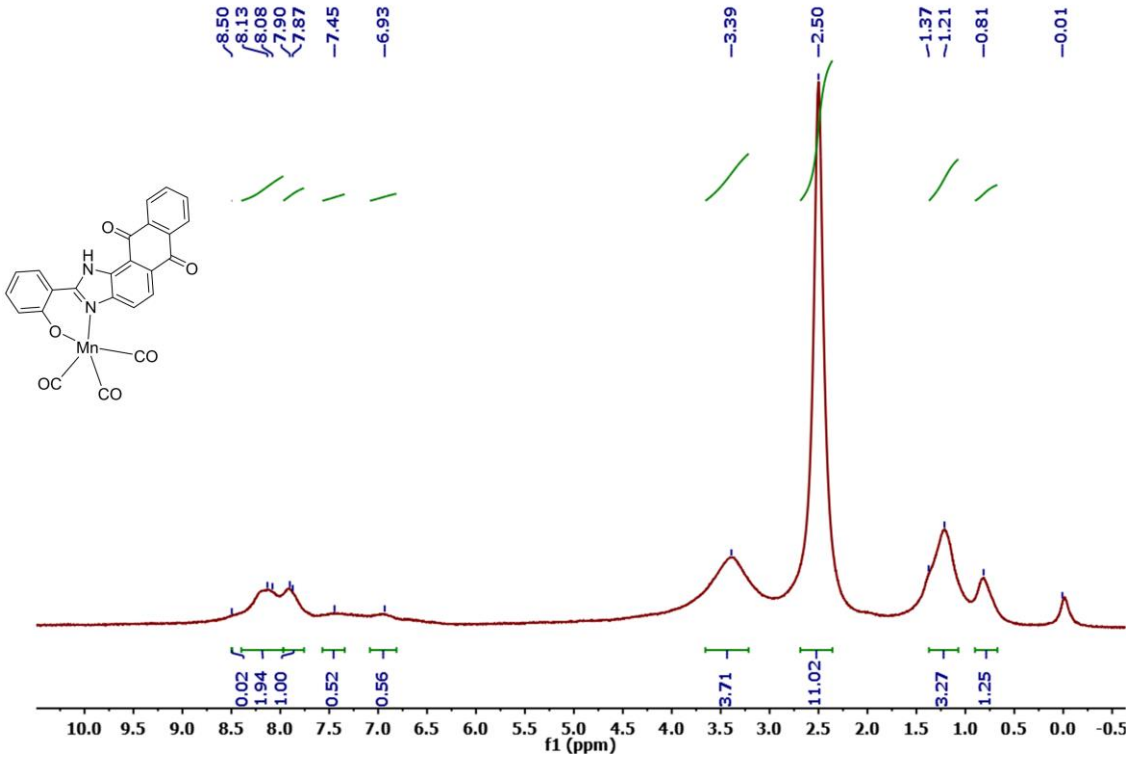

Figure S28.[1]H NMR of **3** recorded in DMSO-d_6 Bruker Avance 400 (400 MHz) spectrometer**.**

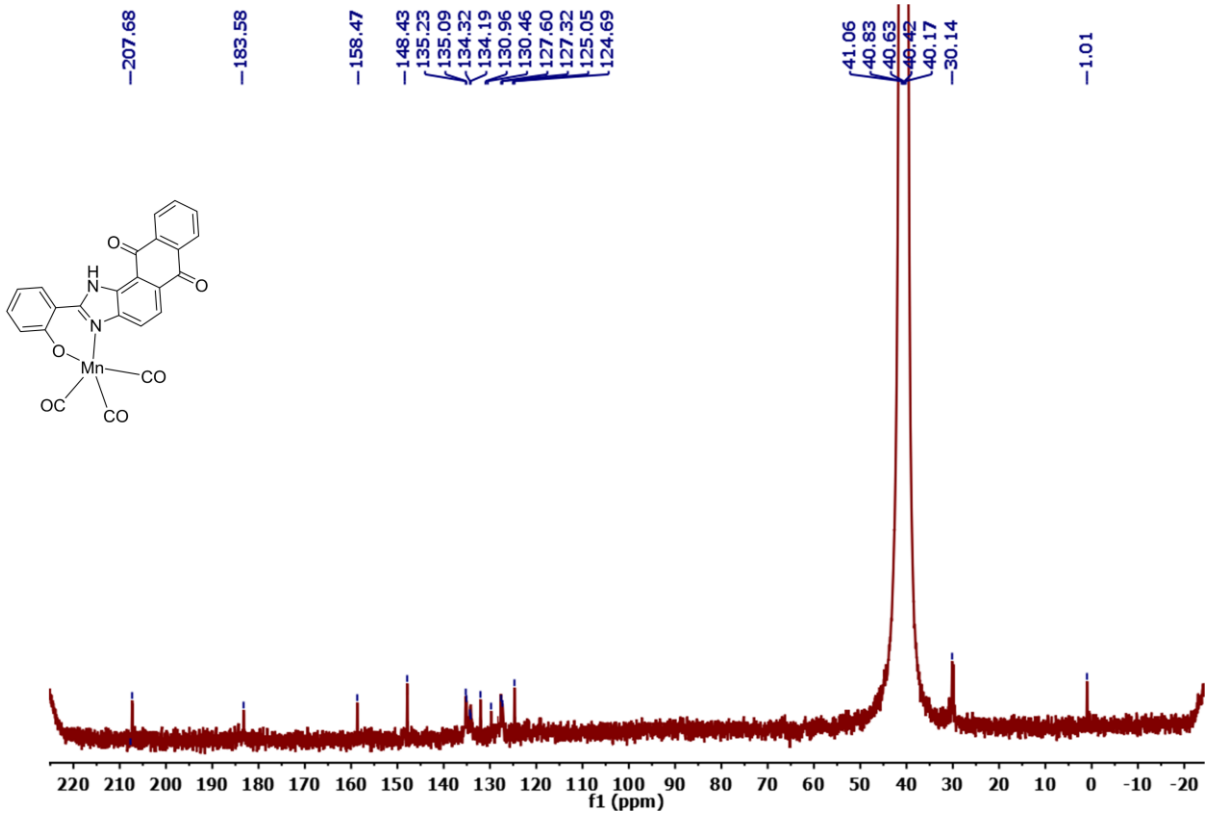

Figure S29.[13]C NMR of **3** recorded in DMSO-d_6Bruker Avance 400 (100 MHz) spectrometer.

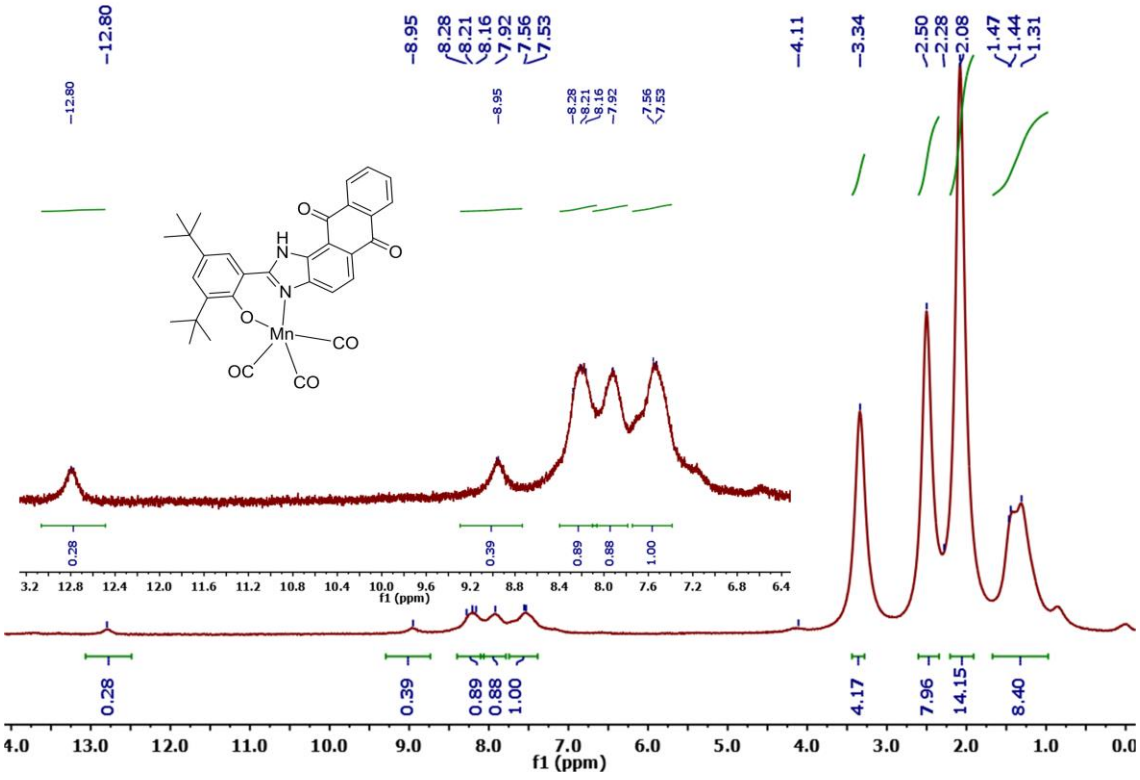

Figure S30.[1]H NMR of **4** recorded in DMSO-d_6 Bruker Avance 400 (400 MHz) spectrometer**.**

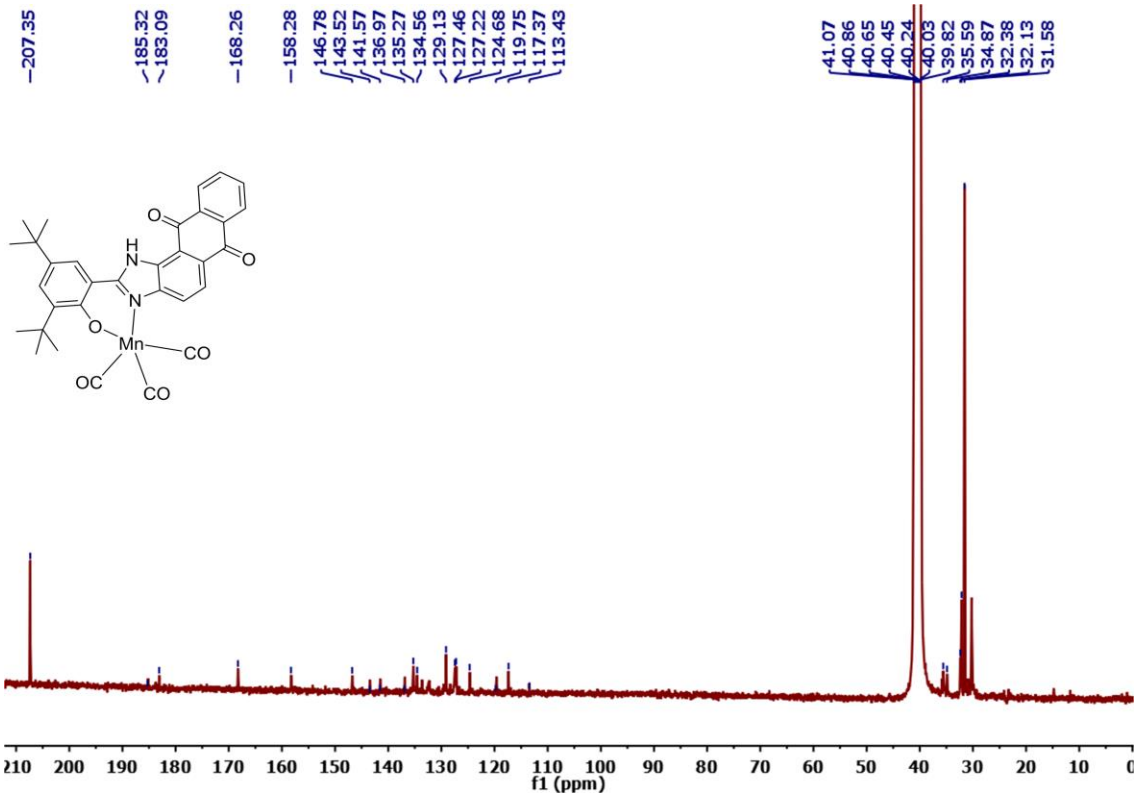

Figure S31. ^{13}C NMR of **4** recorded in DMSO-d_6Bruker Avance 400 (100 MHz) spectrometer.

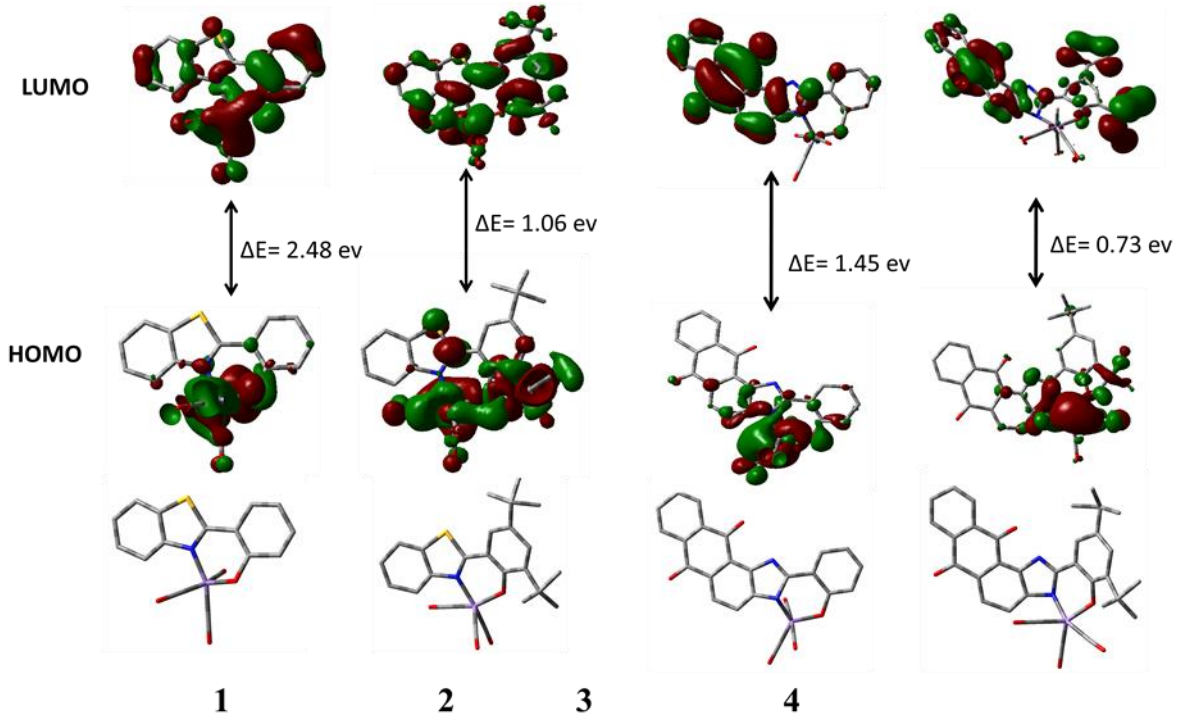

Figure S32. Optimized structure of the complexes (**1-4**) and the corresponding HOMO, LUMO stereographs. Calculated at DFT/B3LYP/6-31G(d,p)/LanL2DZ level in gas phase with Gaussian 09W.

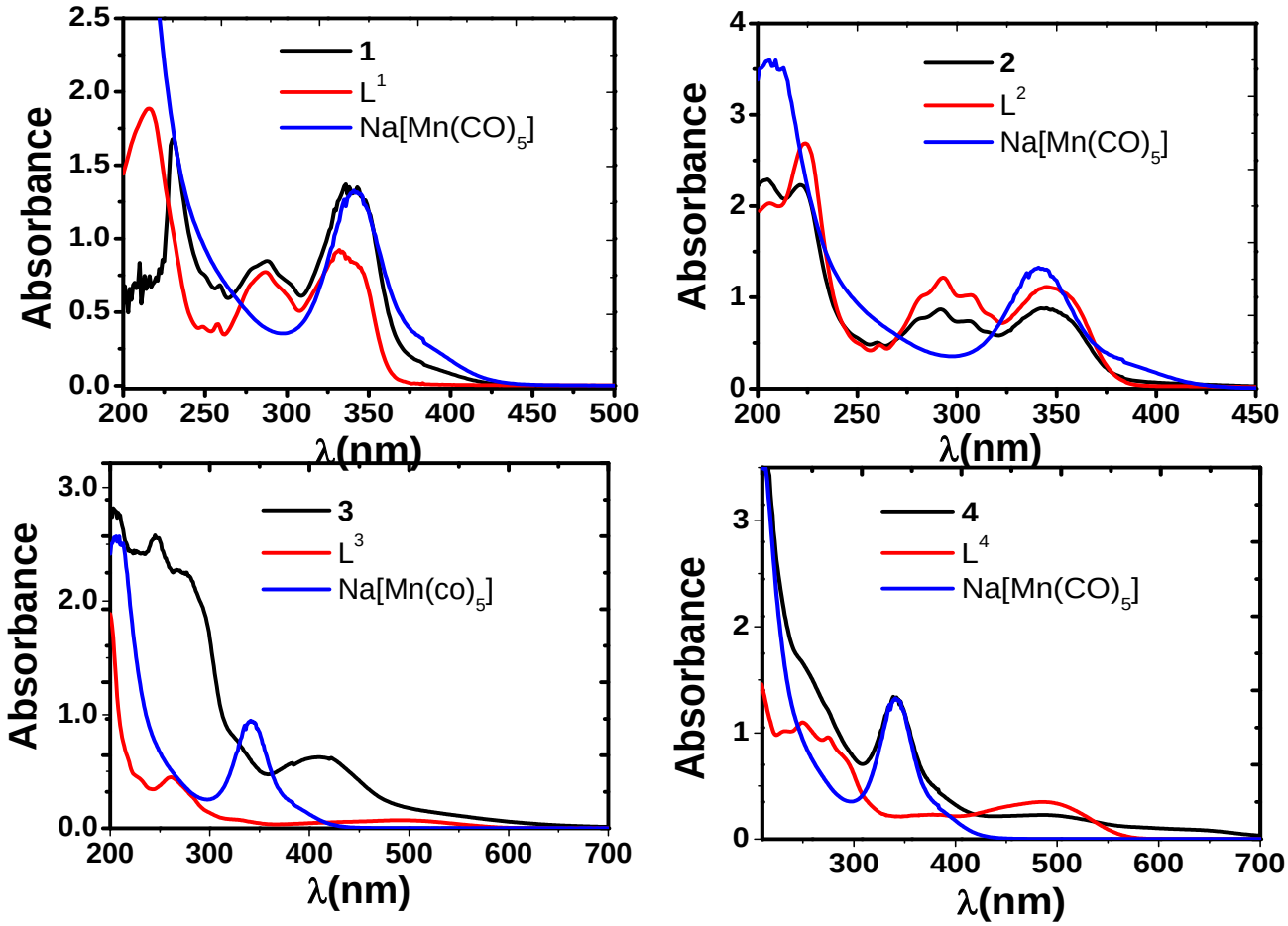

Figure S33. Electronic absorption spectra of $Na[Mn(CO)_5]$, Ligands (100 μM) and metal complexes **1-4** (100 μM). complex (Black line), NaMn(CO)5 (blue line), and Ligand (red line) in MeCN solutions at 298 K. UV-vis. Spectra of $Na[Mn(CO)_5]$ was recorded with unknown concentration since it was generated in situ during preparation of the complexes.

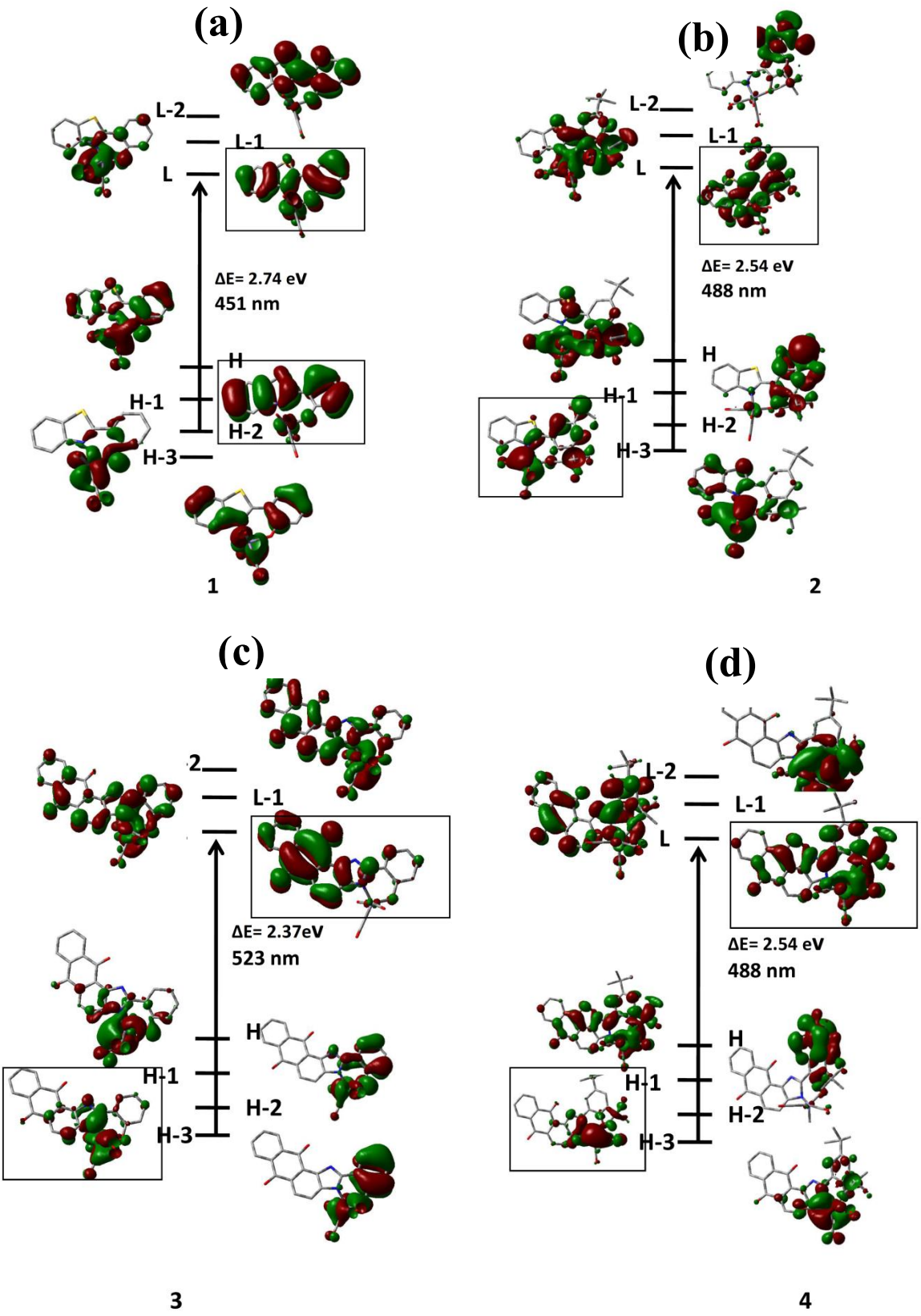

Figure S34. Electronic transitions predicted on the basis of TD-DFT Calculations for **1-4**. calculated at TDDFT/B3LYP/6-31G(d,p)/LanL2DZ level in gas phase with Gaussian 09W.

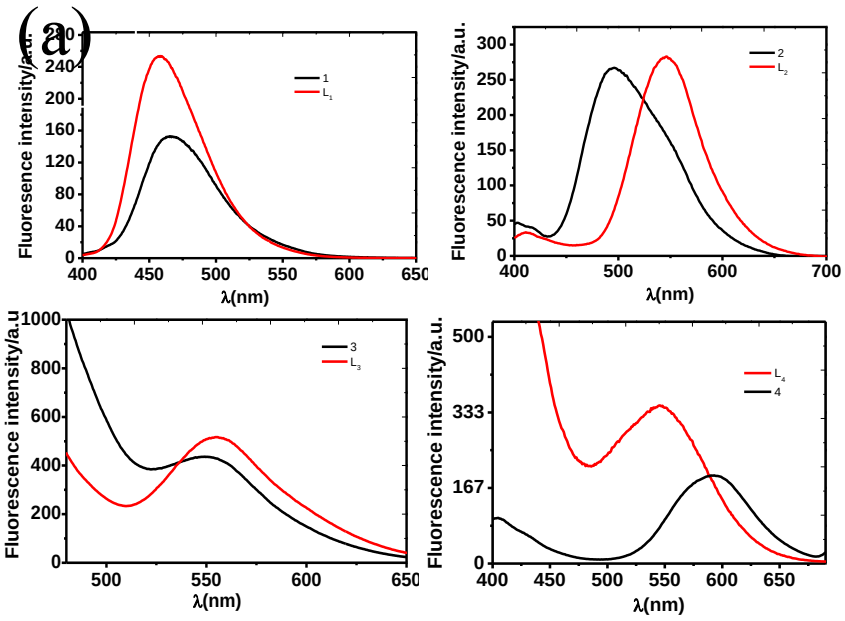

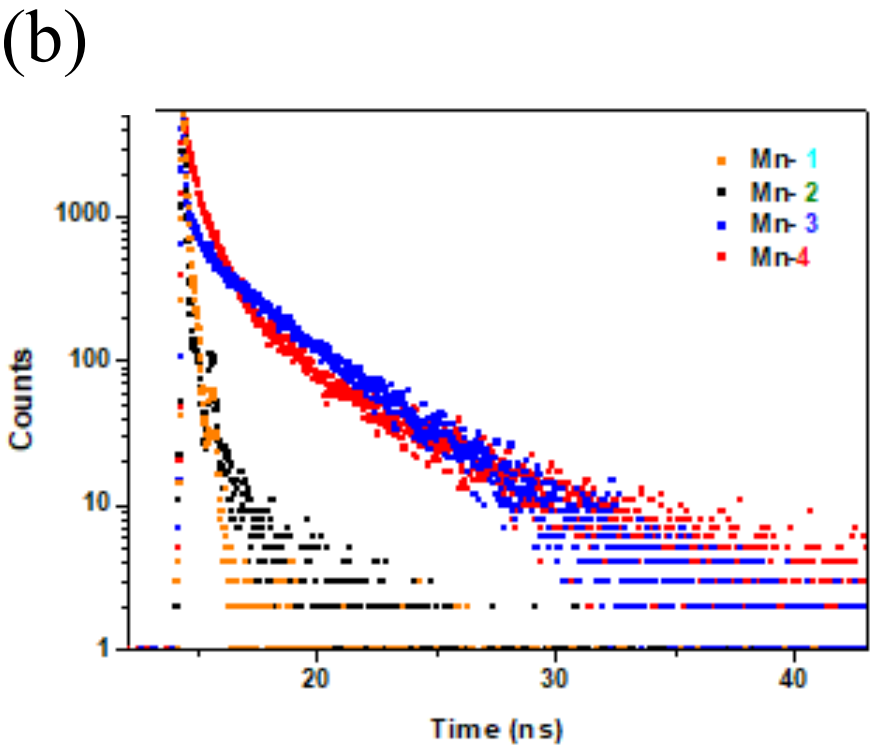

Figure S35. Emission spectra of the ligands (L^1-L^4) (100 μM), complexes **1-4** (100 μM) (λ_{ex}:350nm) and luminescence lifetime of the Complexes (Black line) Ligands (red line) in MeCN solution at 298 K.

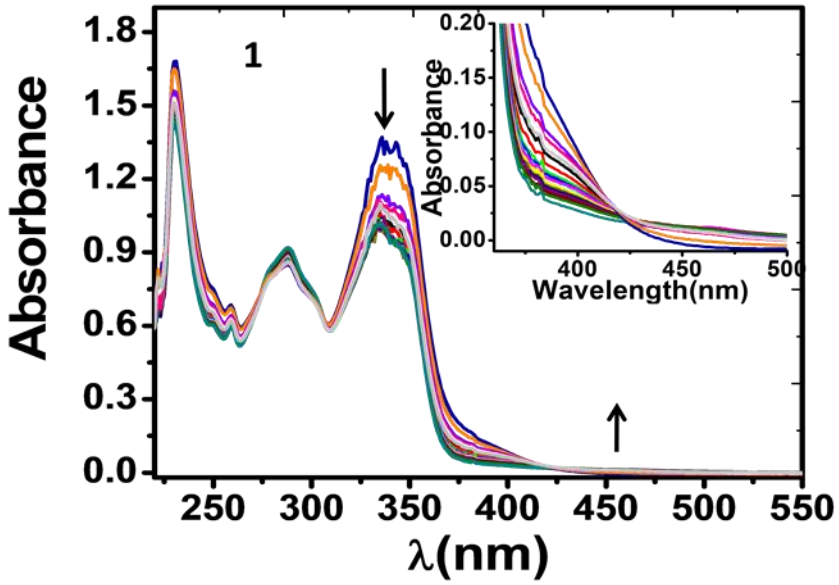

Figure S36. Changes in the electronic absorption spectrum of complex **1** in CH_3CN (0.10 mM) upon exposure to light (λ, 400-700 nm, 10 J cm^{-2}).

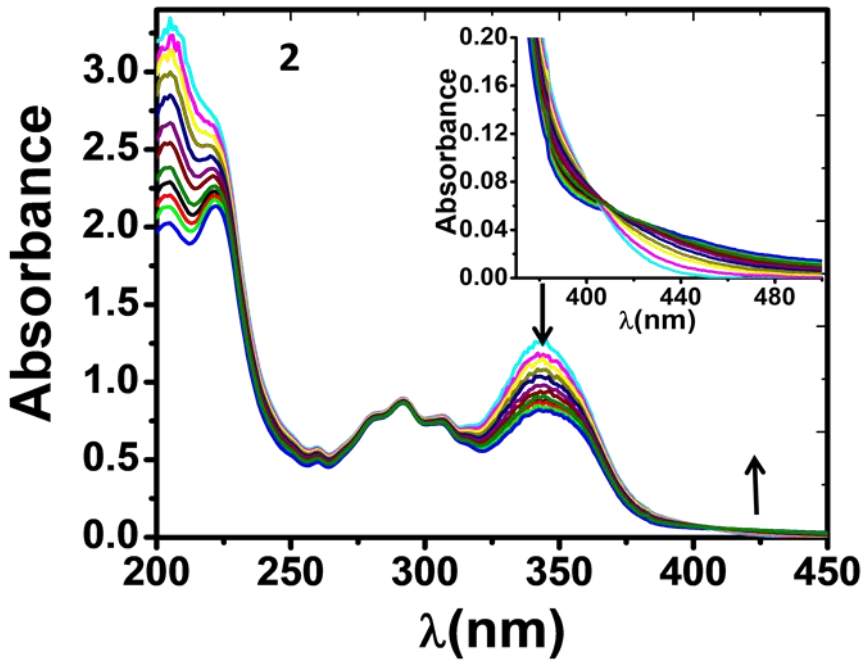

Figure S37. Changes in the electronic absorption spectrum of complex **2** in Ch_3CN (0.10 mM) upon exposure to light (λ, 400-700 nm, 10 J cm^{-2}).

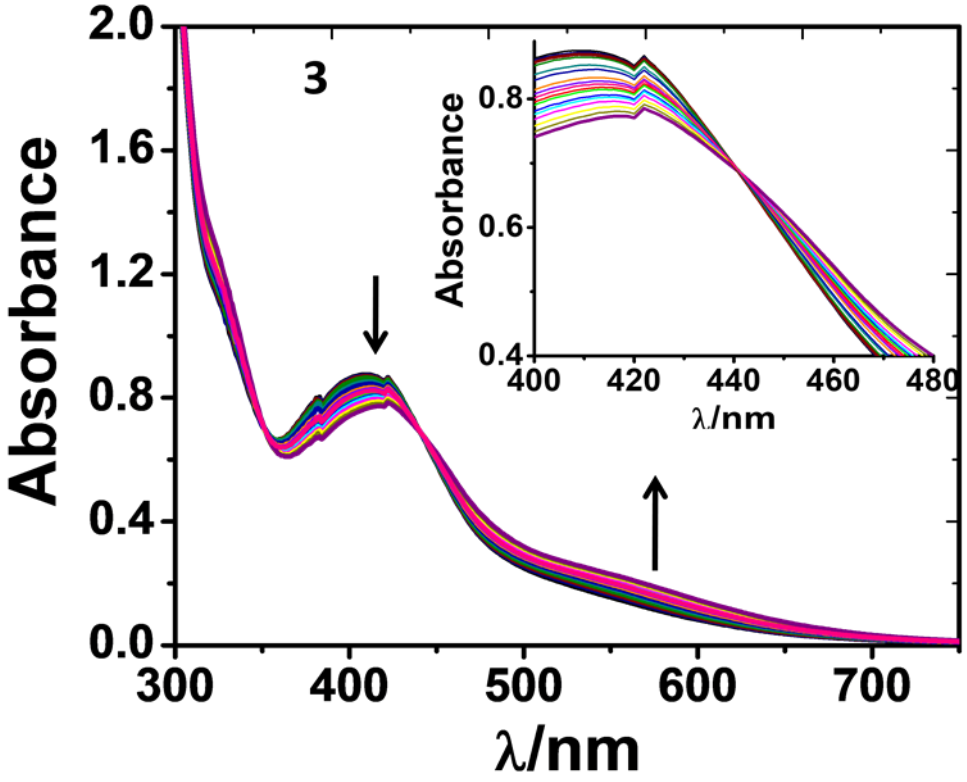

Figure S38. Changes in the electronic absorption spectrum of complex **3** in CH_3CN (0.10 mM) upon exposure to light (λ, 400-700 nm, 10 J cm^{-2}).

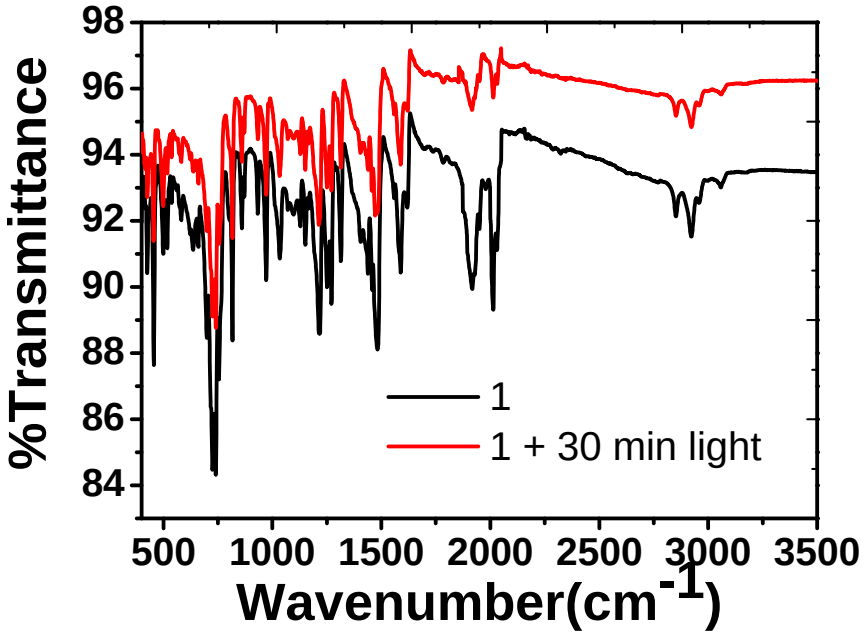

Figure S39. IR spectra of **1** (black line before photolyzed and red line after photolyzed).

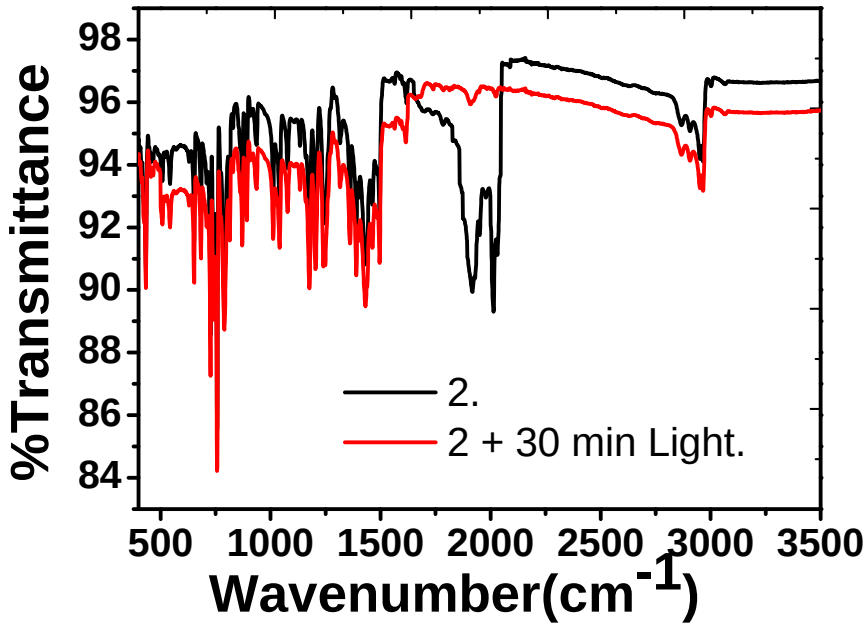

Figure S40. IR spectra of **2** (black line before photolyzed and red line after photolyzed).

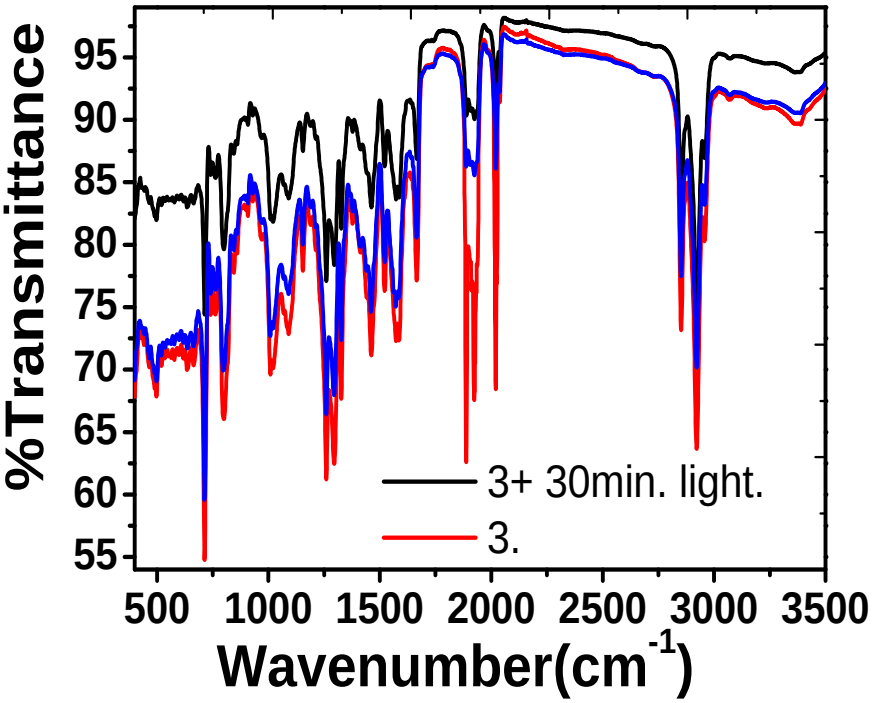

Figure S41. IR spectra of **3** (black line before photolyzed and red line after photolyzed).

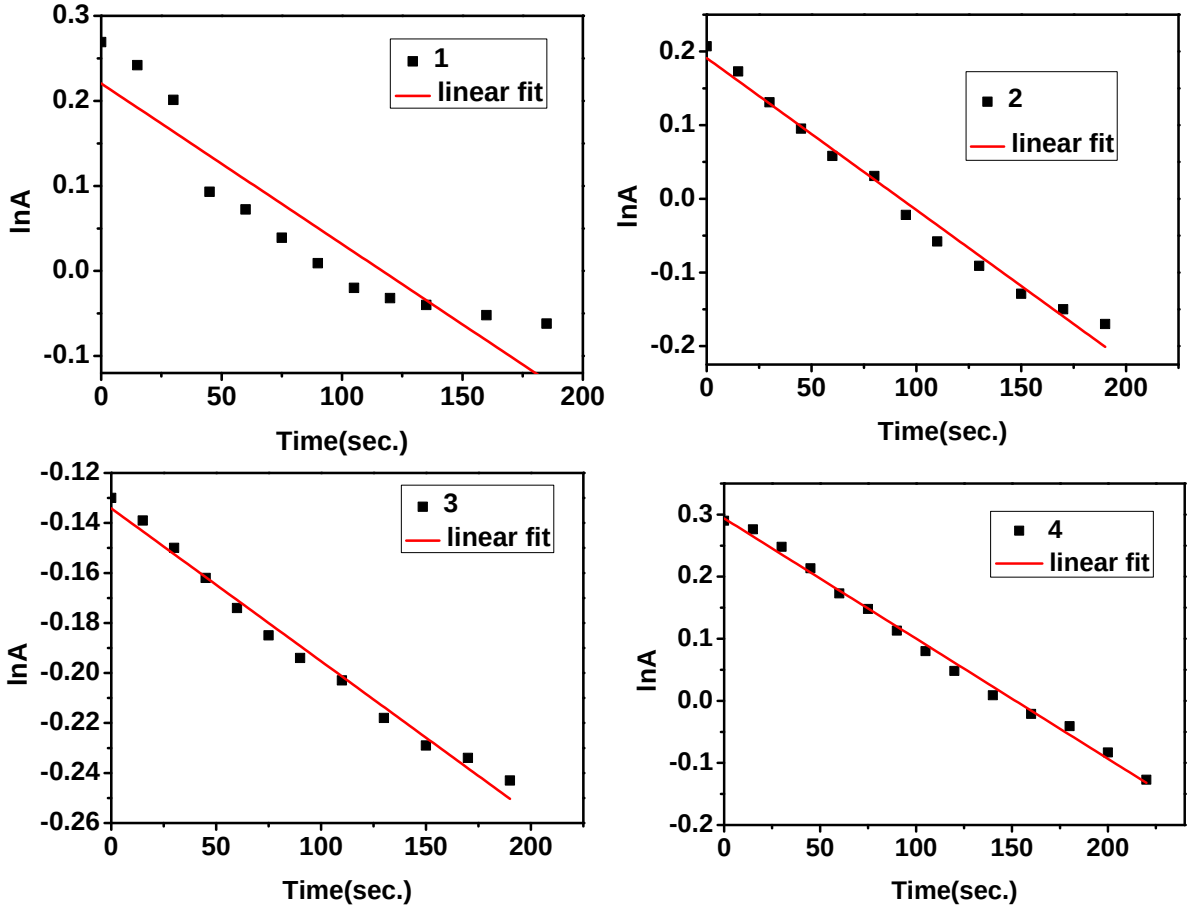

Figure S42. The apparent rate constant determined by linear fit of lnA vs time.

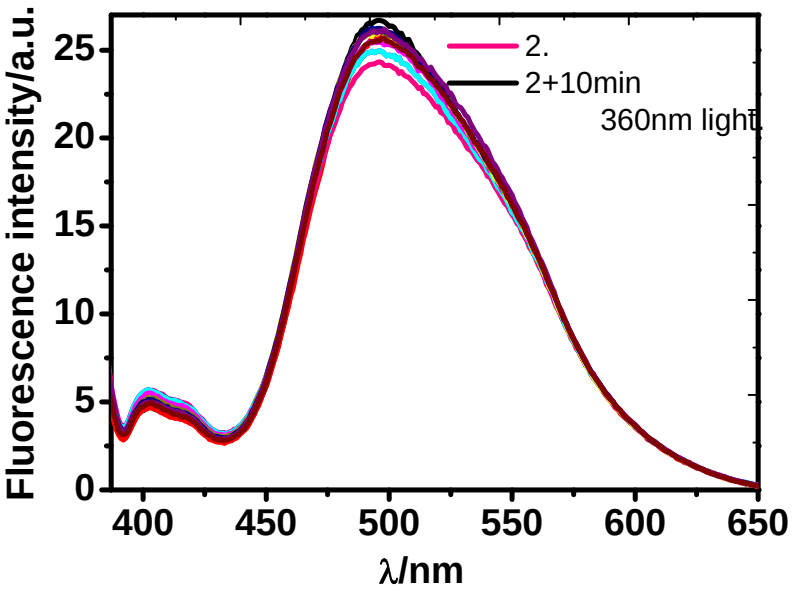

Figure 43. The photolyzed emission spectra of complex **2** (λ_{ex}: 350 nm) in CH_3CN solution recorded for 30 min of visible light irradiation at 298 K.

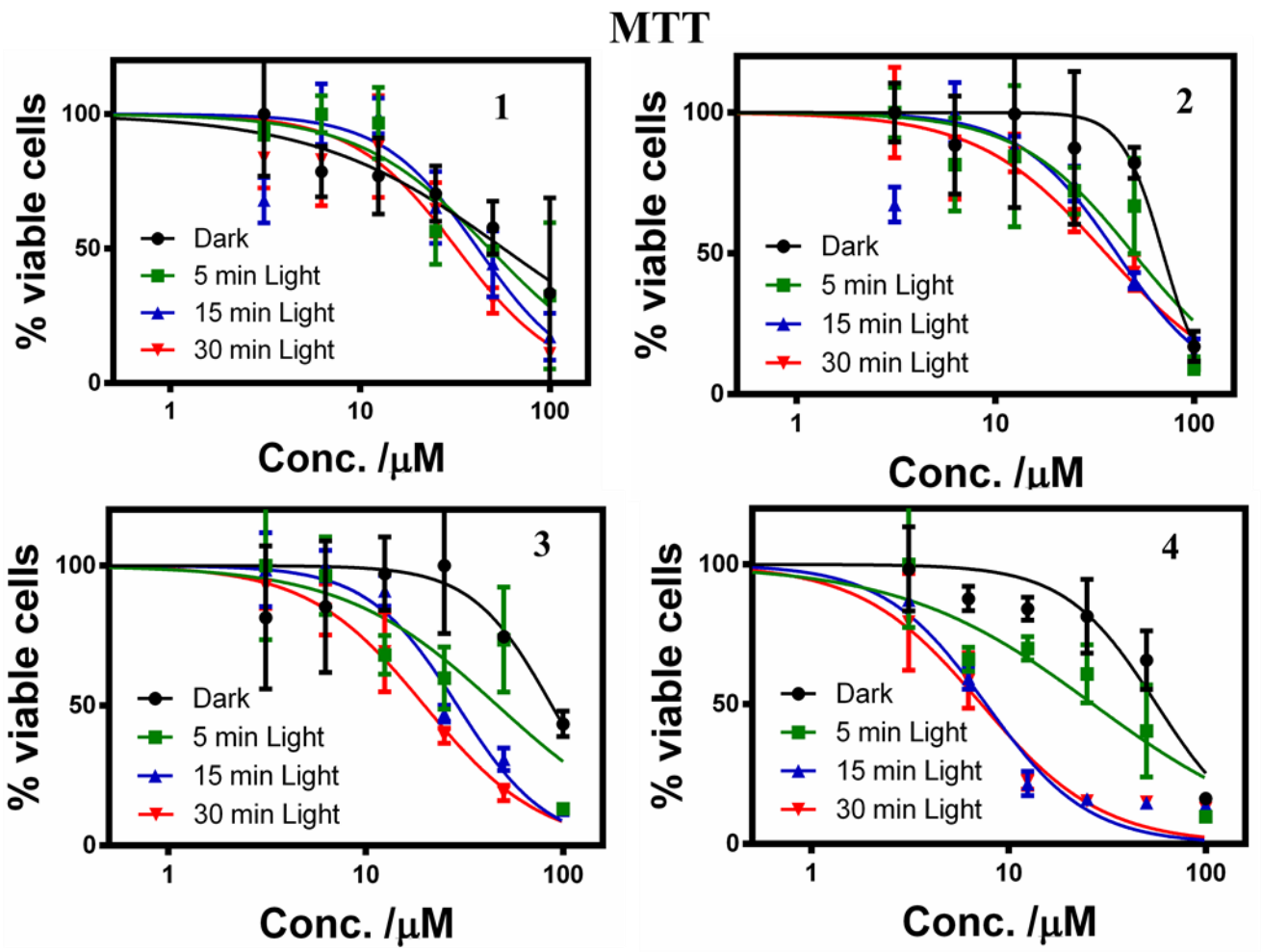

Figure S44. Cell viability (MTT assay) plots showing the cytotoxicity of the complexes (**1-4**).